Gravity Profile Evaluation of Geological Cross-sections through the Southern Appalachians in Frederick County, Virginia

by

Captain Michael Randolph Mason

United States Army Corps of Engineers

Thesis submitted to the Faculty of the

Virginia Polytechnic Institute and State University

in partial fulfillment of the requirements for the degree of

Master of Science, Geophysics

in

Department of Geological Sciences

APPROVED:

Edwin S. Robinson, Chairman

John K. Costain

Cahit Çoruh

June 1, 1989

Blacksburg, Virginia

Gravity Profile Evaluation of

Geological Cross-sections through the

Southern Appalachians

in Frederick County, Virginia

by

Captain Michael Randolph Mason

United States Army Corps of Engineers

Edwin S. Robinson, Chairman

Department of Geological Sciences

(ABSTRACT)

The geology of Frederick County, Virginia is known mostly from surface mapping. Based on this work are interpretations of the subsurface geology including cross sections which have been constrained by the surface geology and by the method of area balancing based upon palinspastic reconstruction. With the intent to further constrain these cross sections, gravity measurements were made at 422 sites in Frederick County. Then, gravity anomalies were compared with theoretical gravity profiles calculated from two dimensional models of density distribution based upon the cross sections.

Using the cross section geometry and densities published for the known and inferred rock units, the theoretical gravity profiles did not compare favorably with corresponding Bouguer gravity profiles. However, by modifying the geometry of the model units and adjusting the model unit densities, a reasonable fit between theoretical and Bouguer gravity profiles was obtained. Although the geometrical modifications adhered to the structural style, no attempt was made to area balance these modifications within the model. Lack of balancing is not necessarily a shortcoming in view of the possibility that volume balance may exist in the third dimension, or that area balance may be possible by modification of other parts of the larger geologic cross section. If the modified model correctly represents the known surface geology and subsurface structural style and produces a profile which reproduces the character of the

Bouguer gravity from the field, then the model represents a viable interpretation in the absence of more focused subsurface information.

It is possible to explain the Bouguer gravity variations in Frederick County in terms of upper crustal features less than 6 km in depth. This is not proof that deeper density contrasts are insignificant or nonexistant, but only shows that they might not be significant.

Acknowledgements

I am thankful for the guidance and encouragement of Dr. Edwin S. Robinson in the conduct of this study and in the pursuit of the academics associated with my graduate studies in geophysics.

Drs. John K. Costain and Cahit Çoruh assisted me in the solution of various technical difficulties and development of computer programs. Dr. Costain and Dr. Çoruh also reviewed the manuscript and made suggestions for enhancement of my work. I wish to express my appreciation to my fellow graduate students who were helpful every step of the way and at all hours of the day.

Dr. Blair Jones of the Virginia Polytechnic Institute and State University Forestry Department provided the digital terrain elevation data for use in the terrain correction program.

I am especially thankful to my wife, , for acting as navigator/recorder during the field work, for assisting me in digitizing data point locations, for editing this manuscript, and for being patient with the time, expense, and occasional frustration.

I wish to acknowledge the United States Army Advanced Civil Schooling program under which I was afforded the opportunity for my graduate education. This research was fully funded by the United States Army in accordance with Army Regulation 621-1.

Table of Contents

List of Figures and Tables

Introduction

Frederick County is the northernmost county in Virginia. Although there is one short seismic line north of Winchester (Evans, 1989), the geology of the county is known mostly from surface mapping, (Butts and Edmundson, 1963). The stratigraphic units and structural features (Figure 1) appear to be typical of the folded and thrust faulted Valley and Ridge terrane in Virginia.

Important structural features that are evident from rocks exposed at the land surface include the Little North Mountain fault which separates the county into two geologically different parts. West of the fault is the Great North Mountain anticlinorium and the Mount Pleasant syncline, and to the east is the Massanutten synclinorium.

Interpretations of the subsurface geology include cross sections (Woodward, 1985) that have been constrained by the surface geology and by the method of area balancing based upon palinspastic reconstructions. The structural style presented in these cross sections is consistent with that of imbricate thrust faults originating along major decollements within the Cambrian-age Rome Formation. These ideas have been confirmed by seismic reflection surveying in the Valley and Ridge province (Evans, 1989). Within Frederick County, there is seismic reflection data along a line, which passes to the north of Winchester, and crosses the Little North Mountain fault and Massanutten synclinorium.

The purpose of this study is to constrain further the interpretations of subsurface geology by means of gravity field measurements. To this purpose, gravity measurements were made at 422 sites in Frederick County. Gravity anomalies calculated from these measurements were then compared with theoretical gravity anomalies calculated from two-dimensional models of density distribution based upon cross sections from Woodward (1985). Then, by means of trial calculations involving changes in the density and geometry, models were obtained with theoretical gravity anomalies which more closely reproduce the measured gravity anomalies. These models provide insight about the constraints on geometry and density of units in an interpretative geological cross section that are imposed by gravity measurements.

Geology

Frederick County is in the Valley and Ridge Province of the southern Appalachians. This province is dominated by folded and thrust faulted sedimentary rocks. The trend of the structures in this region is generally northeast/southwest. In the county are two large structures, the Massanutten synclinorium, on the east, and the Great North Mountain anticlinorium, on the west. The Massanutten synclinorium is thrust onto the Great North Mountain anticlinorium along the Little North Mountain fault, which is exposed along Little North Mountain.

Stratigraphy

The densities of the rock units in the study area are an important factor in the analysis of gravity measurements. The exposed rock units in this area have been mapped and described (Figure 1) by Butts and Edmunson (1963, 1966). The densities of rocks similar to those exposed in the study area have been measured by Edsall (1974) and Kolich (1974) and are presented in Table 1. The following is a discussion of rock units present in Frederick County and how they correlate with rock units elsewhere in the Valley and Ridge Province that were tested by Edsall (1974) and Kolich (1974).

Opequon Creek forms the eastern border of Frederick county. Westward from Opequon Creek to Interstate 81, a distance of 7-10 km, the surface exposures are almost entirely Ordovician age Martinsburg shale (Omb) (Butts and Edmundson, 1963). The Martinsburg shale was deposited in the clastic wedge of a foreland basin formed during the Taconic orogeny of middle to late Ordovician time (Thomas, 1983, and Glover, 1989).

Older rocks bordering the Martinsburg shale on both eastern and western limbs of the Massanutten synclinorium are rocks of the Upper and Lower Knox Groups. From the Upper Knox Group are the Edinburg (Oe) and Lincolnshire (Ol) formations which are dark gray, compact limestones with nodules of black chert and variable amounts of black shale. In the Upper Knox, they are above the New Market (On), Bellefonte (Obe), Nittany (Oni), and Chepultepec (Och) formations of thick bedded limestone and dolomite. (Butts and Edmundson, 1963) Although none is indicated, there may be an unconformity between the Bellefonte and the Martinsburg formations which would represent passage of a peripheral bulge which presaged the oncoming continent of Carolinia and the Taconic orogeny as envisaged for the southern Appalachians by Read, (in press). (Note: Carolinia is also referred to as Avalonia in some interpretations.) The Upper Knox is early Ordovician in age, 505-490 Ma (Read, in press).

The Cambrian time, 570-505 Ma, is represented in the column by the Conococheague (Co) formation of the Lower Knox group and the Elbrook (Ce) formation. The Conococheague formation is mostly limestone with some interbedded gray dolomite and a few beds of coarse grained friable sandstone. The Elbrook formation is composed of thin-bedded, impure limestone and dolomite. (Butts and Edmundson, 1963) The Little North Mountain thrust fault truncates the bottom of the Elbrook formation on the west. Immediately to the west of the Little North Mountain fault is a narrow strip of Martinsburg shale which may indicate that the fault surface is in or on the Martinsburg. There are small fragments of the Juniata and

Oswego sandstones (Ojos) intermittently along the western edge of this outcrop of the Martinsburg. (Butts and Edmundson, 1963)

Lying above the Cambro-Ordovician sequence, are formations that represent the shallow water deposition of the Taconic clastic wedge (Glover, 1989). The Silurian age, 438-408 Ma, Tuscarora (Stu), Clinton (Scl), McKenzie (Smk), Bloomsburg (Sb), and Wills Creek (Swc) formations are interbedded sandstones and shales. (Butts and Edmundson, 1963) The Tonoloway formation (St) of thin bedded limestone with sandy layers represents the beginning of an epicontinental sea following the Taconic orogeny, 490-440 Ma (Glover, 1989).

At the end of the Taconic orogeny a shallow epicontinental sea collected sediments in a low energy environment (Glover, 1989). The rocks which record this period are in the Oriskany sandstone and Helderberg limestone (Dsch). These rocks are further subdivided into the Silurian Keyser (Sk) and Devonian New Scotland (Dns) formations which are limestone, and the Oriskany formation (Do) which is a coarse grained, thick-bedded sandstone. (Butts and Edmundson, 1963)

In early Devonian time, the Acadian orogeny, 408-350 Ma, produced a second clastic wedge (Glover, 1989). The rocks which record the Acadian orogeny are the Onondaga (Don) and Marcellus (Dmr) shale formations. The filling of the Acadian foreland basin is recorded in the Hamilton (Dha), Brallier (Db), Chemung (Dch), and Hampshire (Dhs) formations which are all interbedded sandstones and shales. There is a small exposure of the Mississippian age Pocono (Mpo) shale, sandstone, and conglomerate formation near Shockeysville on the Northern border of the county. (Butts and Edmundson, 1963)

Using stratigraphic columns and tectonic sequences for the Valley and Ridge Provinces of southwestern Virginia of Glover (1989) and Read (in press), equivalent formations tested by Edsall (1974) and Kolich (1974) (Table 1) were chosen to obtain density values for use in analysis of gravity measurements. Where no equivalent was found in Edsall (1974) and Kolich (1974), density values were taken from Kulander and Dean (1972), Byerly (1973), Dean (1966), or Knotts (1984).

Structure

The obvious structures are a major anticlinorium separated from a major synclinorium by the Little North Mountain thrust fault. These three features will be described in the order in which they were formed.

The *Massanutten synclinorium* is a foreland basin formed during the middle Ordovician (490-440 Ma) and filled with clastic wedge sediments eroded from the Taconic melange and adjacent oncoming continent of Carolinia. The sediment source would have been from the direction of what is presently east. The foreland basin was the closing Iapetus Ocean. The sediments and basin were subsequently folded and thrusted by the Alleghanian (340-310 Ma) orogeny. (Glover, 1989)

The *Great North Mountain anticlinorium* is composed of sediments accumulated in an epicontinental sea (440-408 Ma) following the Taconic orogeny, and in the clastic wedge resulting from the Acadian orogeny (408-350 Ma). The folding of the Great North Mountain anticlinorium came about during the Alleghanian orogeny (Glover, 1989).

The *Little North Mountain fault* must be Alleghanian in age as it cuts both depositional environments recorded in the Great North Mountain anticlinorium and the Massanutten synclinorium. The Little North Mountain fault is believed to extend downward into a decollement situated in the Rome shale which is a drift sequence deposit laid down following the opening of the Iapetus Ocean (570-490 Ma). The Rome shale, which is not exposed in Frederick County was deposited on the continent side of a rimmed basin. Therefore, its sediments came from what is presently west (Read, in press).

Deeper structural features inferred from the surface geology in Frederick County are shown on three geologic cross sections (Figure 2) published in Woodward (1985). In the compilation of the three cross sections the geologists used palinspastic reconstructions to balance the cross section areas. In a palinspastic section, the geological structures represented have been restored insofar as possible to their original geographical positions, before the crust was deformed by tectonic activity (Bates and Jackson, 1987). Seismic reflection data has been used by Evans (1989) to support palinspastic reconstruction. The three cross sections illustrate a tectonic style consisting of imbricate faults and folds which are area balanced to be consistent with the palinspastic sections with regard to the total cross-sectional area occupied by each stratigraphic unit. This tectonic style has been verified by seismic reflection profiles in the Valley and Ridge Province. One seismic profile in Frederick County tends to confirm the structural style of the cross sections (Evans, 1989).

The two cross sections prepared by T.H. Wilson (1985, Lines 3 and 5 from Woodward, 1985) display basal Cambro-Ordovician blocks displaced along imbricate thrusts which control the draped surface west of the Little North Mountain Fault. According to Wilson, the presence of these large blocks is inferred from surface exposure and basement depths in this area. The exposures are certainly in other areas as the cross sections show the imbricate blocks approaching no closer than 1.5 km to the surface. Either the Cambro-Ordovician blocks or the Silurian-Devonian units may be thicker; either case could be the result of internal detachment. Both possibilities have been represented on seismic sections in other areas. It is also noted by T.H. Wilson (1985) that gravity anomalies over the western part of the study area are not as high as might be expected. This is attributed to excessive amounts of low density Martinsburg shale obscuring duplications of the Cambro-Ordivician blocks. The lenticular formation in the subsurface east of the Little North Mountain fault is indicated as conjecture based on the shearing off of the Great Valley block. (Wilson, 1985)

The cross section, Line 4, prepared by Knotts and Dunne (1985) does not show the structure in Frederick County to be controlled by imbricate faulting of the Cambro-Ordovician complex. Rather, the North Mountain anticline and its adjacent structures west of the Little North Mountain fault are chiefly the result of imbricate thrust faulting of the Devonian-Ordovician unit. Here the Massanutten synclinorium is thrust upon the Little North Mountain fault by an encroaching wedge of the Blue Ridge Mountain block. This wedge has been forced between the Cambro-Ordovician block of the overlying Massanutten structure and the Cambro-Ordovician Blue Ridge blocks below as if to exploit a weakness within the Rome shale upon which it has been displaced. When compared with lines 3 and 5, it is seen that line 4 represents an alternate interpretation of Valley and Ridge structures in Frederick County which is also consistent with the constraints of surface geology and area balancing.

Gravity

Gravity data used in this study are the results of measurements taken at 422 sites in Frederick County between 7 June, 1988 and 6 July, 1988. The site locations are plotted on Figures 4a and 4b. The latitude and longitude for each site are listed in the appendix. Gravity reading stations were determined from elevations marked on USGS 7.5 minute quadrangles. These locations were mostly road intersections or benchmarks where the elevation accuracy is estimated to be $\mp$ 1 ft ($\mp$ 0.3 m). Where elevation was marked at a bridge abutment or on fill material, the gravity measurement was made nearby on firm ground and an elevation adjustment was estimated. At these sites elevations are estimated to be accurate within $\mp$ 2 ft ($\mp$ 0.6 m). The gravity readings were taken using LaCoste-Romberg gravimeter No. G-612 with an accuracy of 0.02 mgal.

Frederick County is 433 sq mi (1121 km^2) in area. Therefore, the coverage is close to one reading per square mile, with an average separation of 5400 ft (1646 m). The coverage is denser in the northern and eastern portions of the county and sparser in the southwestern quarter where mountainous terrain and few roads limit accessibility.

A temporary base station was established at the corner of West Whitlock Avenue and Ivy Street in Winchester, Virginia by means of gravimeter ties to the established Virginia Tech

Gravity Base Station at Derring Hall in Blacksburg, Va. At all observation sites, relative gravity values were calculated from gravity meter dial readings using the instrument calibration table in the instrument user's manual.

A reading was taken at the temporary base station at the start and end of each day of field surveying. Using the base station readings, instrument drift was removed from each field station reading through application of a time dependent linear drift correction. Lunar/solar tide corrections were applied using the equations of Longman (1959) with a solid earth tidal gravity factor of 1.16 (Robinson, 1974). After making these corrections, the relative gravity values of the field stations were adjusted to the observed gravity value at the Winchester base station.

The temporary Winchester base station gravity value was calculated to be 979985.94 mgal. This value was determined from gravimeter ties to the Derring Hall station in Blacksburg, Virginia which, in turn, was tied to the National Geodetic Survey absolute gravity base station in Blacksburg, VA, where falling mass measurements made in July, 1987 and May, 1988 indicated an absolute gravity value of 979715.723 mgal (Moses, 1988).

Gravity measurements were reduced using conventional methods to obtain values of free-air and Bouguer gravity. The formula used to calculate free air gravity, Δg_{fa}, is as follows (Robinson and Çoruh, 1988):

$$\Delta g_{fa} = g_{obs} - (g_t - 0.09406h) \quad (1)$$

and the formula for complete Bouguer gravity, Δg_B, is (Robinson and Çoruh, 1988):

$$\Delta g_B = g_{obs} - (g_t - 0.09406h + 0.01278\rho h - TC) \quad (2)$$

where:

g_{obs} is the observed gravity in mgal

g_t is normal gravity in mgal

h is elevation in feet above mean sea level (MSL)

ρ is density in gm/cm^3

TC is the terrain correction in mgal.

Normal gravity, g_t, was calculated using the GRS-67 formula (Woollard, 1979). Following common convention, a density, ρ, of 2.67 gm/cm^3 was applied in the Bouguer and terrain corrections. Gravity values and positions of observation sites are given in the appendix.

The vertical line approximation method was used to calculate terrain corrections (Stovall and others, in press). Blair Jones of the VPI & SU School of Forestry and Wildlife Resources provided an elevation grid which covered the study area with additional surrounding coverage. The grid intervals were 1/3 km (1094 ft). This grid is part of the coverage of the entire Commonwealth of Virginia. The terrain is represented by the average elevation within each grid cell. The mass of the terrain within the grid cell is reduced to a vertical line at the center of the cell. The gravitational attraction at the gravity measurement site of that vertical line is calculated, and the attractions of all cells within an effective distance are summed to yield the terrain correction, TC. The effective distance was chosen to be 15,000 ft (4,572 m).

The accuracy of the station elevation is of central importance to the accuracy of Bouguer gravity values. Using a density of 2.67 gm/cm^3 in Equation (2), it can be determined that an elevation uncertainty of 1 foot yields a Bouguer gravity uncertainty of 0.06 mgal. Since the expected error in elevation for the field survey in this study is $\mp$ 2 feet, the effect of elevation on the precision of the Bouguer gravity values is $\mp$ 0.12 mgal.

Bouguer gravity accuracy is also dependent on the precision of terrain corrections. Comparison of terrain corrections obtained by the method of Hammer (1939) and by the vertical line approximation method (Stovall and others, in press, and Moses, 1988) indicated that a value obtained by the latter method is generally accurate within 25 percent of the total terrain correction. In Frederick County, the terrain corrections east of the Little North Mountain fault are mostly smaller than 0.23 mgal which introduces a corresponding uncertainty of approximately 0.06 mgal in the Bouguer gravity values. West of the Little North Mountain fault, the terrain is more rugged. Here the average terrain correction is 0.75 mgal, and a few values exceed 4 mgal. Therefore the Bouguer gravity values have correspondingly larger uncertainties in the western part of the study area than exist east of the fault.

Using the GCONTOUR routine available from the SAS Institute of Cary, NC, (SAS, 1985), the complete Bouguer gravity values for all stations were plotted and contoured. The Bouguer gravity contour map (Figure 3) shows that the Bouguer gravity ranges from -65 to -57 mgal. The anomaly patterns are consistent with the NE-SW structural trends of the Appalachians in the study area.

Regional Field

The Bouguer gravity field consists of superimposed anomalies from many sources. Anomalies of local extent are produced by relatively shallow sources, but the broader regional anomalies can be produced by deep as well as shallow sources. Ideally, it would be desirable to separate gravity contributions of deep sources from those of shallow sources. However, this is impossible to accomplish through analysis of gravity data alone (Robinson and Çoruh, 1988). In the absence of independent information, the judgement must be subjective. In analyses of gravity surveys in other parts of Virginia, Sears and Robinson (1971), Keller and others (1985), Stovall and others (in press), and Moses (1988), all concluded that Bouguer gravity variations in their survey areas could be attributed entirely to some combination of change in crustal thickness and density contrasts within the upper 10 km of the crust. In each of these studies, the effect of crustal thickness could be represented by either a plane polynomial function or a quadratic polynomial function. These polynomial functions were determined from Bouguer gravity values by the method of least squares. Regional gravity variations represented by the polynomial functions were observed to be consistent with gravity variations related to crustal thickness changes determined from seismic refraction measurements (James and others, 1968).

The regional gravity field in Frederick County was investigated by the same method used in these earlier studies. First it was assumed that the regional field could be represented by a plane polynomial of the form:

$$g_r(x,y) = Ax + By + C \tag{3}$$

where g_r is the regional gravity value at longitude x and latitude y (degrees), and A,B, and C are constant coefficients (Moses, 1988).

The 422 Bouguer gravity values from Frederick County were used to find the coefficients of this plane polynomial by means of the SAS plane fitting routine, PROC REG. The routine interpolates the Bouguer gravity values at intersections on a square grid. The grid interval is chosen by the user. The method used is bicubic spline interpolation. Then, using the method of least squares, the program fits a plane polynomial function to the grid intersection values. The fitted plane is returned to the user as a contour map (Figure 4a) of the regional field which graphically displays the orientation and gradient of that field.

Examination of the contour map showed a gradient of -0.0075 mgal/km in a N65E direction. Although the direction of this small gradient is quite different from the trend of surface geologic features, it cannot be necessarily concluded that there is insignificant upper crustal influence on the gradient. Because the gradient is small, it would seem that there is no convincing evidence of any important regional gradient associated with either upper crustal geology or variations in crustal thickness. That is to say that the pattern of anomalies viewed on the contour map of Bouguer gravity values in Frederick County (Figure 3) is essentially due to variations in the upper crust.

Next a quadratic polynomial of the form:

$$g_r(x,y) = Ax + By + C + Dx^2 + Exy + Fy^2 \tag{4}$$

was fitted to the grid of Bouguer gravity values by means of the SAS routine PROC RSREG. The result (Figure 4b) indicates a curved regional field oriented along structural trends in the study area, which suggests a dominant upper crustal effect. There is no feature of the quadratic polynomial that clearly can be attributed to variations in crustal thickness or deep crustal anomaly sources. This tends to confirm that the contoured Bouguer gravity anomalies (Figure 3) are almost entirely related to the structure of the upper crust in the study area.

Upper Crustal Anomaly Sources

The upper crustal structural features in Frederick County appear to be the result of overthrusting and folding consequential to tectonic stress from what is now east. At depth, the thrust faults are believed to merge into a master decollement situated in the Rome shale. Below this is the Grenville complex of the Precambrian continent of Laurentia. Seismic reflection studies conducted in northern Virginia support this interpretation (Evans, 1989). The upper surface of the Grenville complex is shown in Figure 2 at approximately 6 km below present mean sea level along Line 4 and at approximately 5 km along Lines 3 and 5. Seismic reflection interpretation in Evans (1989) places the top of the Grenville complex at 5-7 km. For lack of any information about deeper structures, the following analysis of Bouguer gravity is concerned with possible density contrasts associated with rock units lying above the master decollement. The three cross sections in Figure 2 are the most current interpretations of the upper crustal structure in Frederick County. These cross sections provide the basis for preparing interpretive models of gravity anomaly sources.

Analysis

Analysis of Bouguer Gravity Anomalies

Some qualitative correlations of gravity anomalies and geologic features are evident from examination of Figures 1 and 3. Along the axis of the Massanutten synclinorium, where the Martinsburg formation is exposed, Bouguer gravity is relatively high compared with the field over older rocks exposed along the western limb of the synclinorium. Farther west, the Bouguer gravity field is relatively high over the Great North Mountain anticlinorium, but diminishes to the north where the plunge of the structure increases.

Quantitative analysis of the Bouguer gravity field in Frederick County is concentrated on anomalies along the profiles of the three geologic cross sections (Figure 2). This analysis consists of comparisons between the observed gravity variations and theoretical gravity variations calculated using two dimensional models based upon those geologic cross sections.

Bouguer gravity profiles were prepared for lines corresponding to each of the geologic cross sections, and for additional parallel lines offset by 1 km on both sides. Along each of these lines (Figure 3), Bouguer gravity values at intersections with the contours were plotted to obtain the profiles in Figure 5. The reason for preparing a set of three profiles parallel to each geologic cross section is to provide some indication of local gravity variation along the strike of the principal structural features. The differences between the three parallel profiles in each set are the result of departures of the actual anomaly sources from idealized two dimensional structures used to represent these sources.

Theoretical gravity profiles were calculated from two dimensional models for comparison with the Bouguer gravity profiles. The calculations were done by means of a FORTRAN program based upon the familiar line integration method of Talwani and others (1959).

The two dimensional models were developed by the trial and error method using forward modelling. In a series of trial calculations, the densities and shapes of the model units are altered until a theoretical gravity profile is obtained that compares favorably with the measured gravity profiles. This was done in a three step procedure for each set of parallel profiles.

In the first step a model was prepared by choosing polygonal model units with boundaries closely matching boundaries of units shown on the geologic cross sections. For each polygon the density was taken from values measured by Edsall (1974) or Kolich (1974) and an estimate of the proportions of the different stratigraphic units represented by that polygon.

In the second step, the original geometry of the model units was retained, but densities were changed in a series of trial calculations until a corresponding theoretical gravity profile reasonably similar to the observed profiles was obtained. In this step, densities were not constrained to conform with measured values.

The third step involved making reasonable modifications to the geometry of model units to mitigate the largest of the disparities discovered in the first step and then making justifiable modifications to the densities to achieve correspondence between the measured and theoretical gravity profiles. No attempt was made to maintain area balance in making these geometry modifications. Such balancing might be done elsewhere in the total cross section or in the strike direction as volume balancing. Typically, three or four iterations of geometry modification were required to obtain approximate agreement between the profiles, followed by ten to twenty iterations for density modification. Justifiable density values are those values attributable to a lithology and found in the literature. Tables 2, 3, and 4 give the values and citations for densities used in the first and third steps of this analysis.

For each set of profiles, after completion of each of the steps, the departure of the theoretical gravity profile from the Bouguer gravity profiles was observed at 2 km intervals along the profiles. From these observations a value for mean deviation was calculated for each set of profiles. These values are useful for describing how closely the theoretical profiles reproduce the features of the Bouguer gravity profiles.

There was some effort made to reach a density correspondence among common lithological units of the lines. However, this proved to be unmanageable and no correspondence between lines was achieved.

Results of the three step evaluation for each set of profiles are described separately in the following discussion.

Line 3

In the analysis of profiles along line 3 the results of step 1 (Figure 6) show that, except in the area of the Great North Mountain anticlinorium approximately 20 km from the west end of the line, there was poor correspondence between the Bouguer and model profiles. The initial mean deviation was 1.15 mgal. There appears to be a mass deficiency in the area west of Great North Mountain, which, under Line 3, has plunged beneath the surface. Above the Little North Mountain fault, the deviation between Bouguer and model profiles indicates that the model has a mass excess. Over the Massanutten synclinorium, the model is again deficient in mass.

In step 2 (Figure 7) increasing the mass of the Cambro-Ordovician blocks (Oe-Ce) beneath the Great North Mountain synclinorium did not produce a sufficient gravity increase in the model profile to achieve good correspondence. Any additional manipulations of polygon masses degraded the correspondence directly over the axis of the anticlinorium. The disparity proximate to the Little North Mountain fault was improved by reducing the densities of the formations labelled Ce, Ch, and O-S. Correspondence in the area of the Massanutten synclinourium was also improved by increasing the density of the Cambro-Ordovician unit (Oe-Ce) beneath the Martinsburg shale (Omb). The mean deviation after step 2 decreased to 0.64 mgal.

In step 3 (Figure 8), smoothing of the upper geometry of the Cambro-Ordovician blocks and the overlying draped syncline, and geologically justifiable manipulation of the densities in the area of the Great North Mountain synclinorium resulted in additional improvement in the correspondence for the western half of the cross section. Slight improvement was made over the Massanutten synclinorium by increasing the densities of the upper Knox formations (Oe-Ce) and Martinsburg shale (Omb) and decreasing the densities of the lower Knox formations (Ce and Ch). The mean deviation after step 3 was reduced to 0.48 mgal.

Line 4

In the analysis of profiles along Line 4 application of step 1 (Figure 9) resulted the discovery that the model profile was markedly different from the Bouguer gravity profiles. The mean deviation was 2.10 mgal.

Better correspondence was achieved in step 2 (Figure 10) by increasing the density of the Ordovician-Devonian unit (Do-Oo) while decreasing the density of the units labelled (Dh-Don). The reduction of the densities of the lower Knox Elbrook (Ce) and Conococheague (Cco) to 2.68 gm/cm^3 and 2.65 gm/cm^3 respectively, resulted in some improvement, but is difficult to justify from actual density measurements. The mean deviation after step 2 was reduced to 0.42 mgal.

In step three (Figure 11), the opportunity for varying geometry was limited by the smaller number of descrete polygons to choose from. However, approximate correspondence was achieved by creating an imbricate fault structure in the Cambro-Ordovician block (Oe-Ce) beneath the Great North Mountain anticlinorium, replacing the lower density Ordovician-Devonian (Do-Oo) with higher density Oe-Ce material. The density of the Oe-Ce block in the Massanutten synclinorium was reduced as well as the densities of the lower Knox Ce and Cco. A mean deviation of 0.57 mgal was obtained for step 3.

Line 5

The step 1 analysis of Line 5 (Figure 12) revealed fairly good correspondence except over the Little North Mountain fault zone where the model profile departs widely from Bouguer gravity profiles. The mean deviation was 1.44 mgal.

Unreasonably low densities above the Cambro-Ordovician blocks were required in step 2 (Figure 13) to attain even a crude similarity in the profile anomalies. The profiles appeared to be out of phase with each other. A very poor mean deviation of 1.46 mgal resulted from step 2. No way could be found to reconcile the Bouguer and theoretical gravity profiles while retaining model units with this geometry.

In step 3 (Figure 14), the entire top of Cambro-Ordovician block Oe-Ce(b) was removed, replaced with low density Ordovivcian-Silurian (O-S) material, a minimal density for the Martinsburg shale decollement was selected from Knotts (1984), and a wedge of block Oe-Ce(c) was removed. The resulting mean deviation was reduced to 0.33 mgal.

Conclusions

Knowledge of the geology of the Frederick County, Virginia has come mostly from surface mapping (Butts and Edmundson, 1963). Interpretations of the subsurface geology include cross sections (Woodward, 1985) which have been constrained by the surface geology and by the method of area balancing based upon palinspastic reconstruction. These cross sections present a tectonic style that is consistent with the concept of thin skin tectonics involving imbricate thrust faults originating along a major decollement within the Rome formation. These ideas are supported by seismic reflection surveying in the Valley and Ridge province including Frederick County. With the intent to further constrain the area balanced cross sections with gravity measurements, anomalies calculated from field measurements were compared with theoretical gravity anomalies calculated from two dimensional models of density distribution based upon the cross sections.

Using the cross section geometry from Woodward (1985) and densities primarily from Edsall (1974) and Kolich (1974), the theoretical gravity profiles did not agree with Bouguer gravity profiles from field gravity measurements. However, by modifying the geometry of the model units and manipulating the model unit densities, a reasonable fit between theoretical and Bouguer gravity profiles can be obtained. Although the geometry modifications adhered to the structural style, no attempt was made to area balance such modifications within the model. Lack of balancing is not necessarily a shortcoming in view of the possibility that volume balance may exist in the third dimension, or that area balance may be possible by modification of other parts of the larger geologic cross section. In the study area, differences in the three geologic cross sections indicate significant changes along regional strike. Investigation of the three parallel Bouguer gravity profiles drawn along the path of each cross section also showed significant lateral variation. It is therefore necessary to consider the third dimension for volume balancing requirements. Such lateral variations also point out the impracticability of attempting to manipulate a two dimensional model for a perfect fit between theoretical gravity and Bouguer gravity, which is produced by anomaly sources that are not ideally two dimensional.

Where there is a mismatch between field and model profiles, it is commonly accepted that field data represents the true in situ condition and that the geological interpretation requires modification. If the modification to the model is consistent with surface geology and subsurface structural style, comes within reasonable expectations for area or volume balancing, and produces a profile which achieves acceptable agreement with Bouguer gravity, then the model represents a viable interpretation in the absence of more focused subsurface information. It is suggested herein that no geologic cross section should be considered correct unless it is also gravity balanced. If there is a significant difference between the geologic interpretation and the calculated Bouguer gravity that cannot be ascribed to three dimensional effects, then the geological interpretation is probably incorrect.

It is possible to explain the Bouguer gravity variations in Frederick County in terms of upper crustal features less than 6 km in depth. This is not proof that deeper density contrasts are insignificant or nonexistent, but only shows that they might not be significant.

Bibliography

Bates, R.L., and Jackson, J.A. (eds), 1987, *Glossary of Geology* , Third Edition, American Geological Institute, Alexandria, Virginia.

Byerly, J.R., 1973, MS Thesis, "A Gravity Survey of the Great Valley and Little North Mountain in Berkley County, West Virginia", West Virginia University, Morgantown.

Butts, C., and Edmundson, R.S., 1963,*Geologic Map of Frederick County*, Virginia Division of Mineral Resources, Charlottesville.

Butts, C., and Edmundson, R.S., 1966, *Geology and Mineral Resources of Frederick County*, Bulletin 80, Virginia Division of Mineral Resources, Charlottesville.

Calver,J.L., and Hobbs,C.R.B., Jr., editors, 1963, *Geological Map of Virginia*, Virginia Division of Mineral Resources, Charlottesville.

Dean, S.L., 1966, Ph.D Dissertation, "Geology of the Great Valley of West Virginia", West Virginia University, Morgantown.

Edsall, R.W., 1974, MS Thesis: "A Seismic Reflection Study over the Bane Anticline in Giles County, Virginia", Virginia Polytechnic Institute and State University, Blacksburg.

Evans, Mark A., 1989, "The Structural Geometry and Evolution of Foreland Thrust Systems, Northern Virginia", in *Geological Society of America Bulletin*, Vol. 101, pp. 339-354.

Glover, Lynn, III, 1989, "Tectonics of the Virginia Blue Ridge and Piedmont: Field Trip T363", 28th International Geological Congress, Virginia Polytechnic Institute and State University, Blacksburg.

Hammer, Sigmund, 1939, "Terrain Corrections for Gravity Meter Stations", *Geophysics*, Vol. 4, pp. 184-194.

James, D.E., Smith, T.J., and Steinhart, J.S., 1968, "Crustal Structure of the Middle Atlantic States", *Journal of Geophysical Research*, Vol. 73, No. 6, pp. 1983-2007.

Keller, M.R., Robinson, E.S., and Glover, L., 1985, "Seismicity, Seismic Reflection, gravity, and Geology of the Central Virginia Seismic Zone", Part 3, Gravity, *Bulletin of the Geological Society of America*, Vol. 96, No. 12, 7p.

Kolich, T.M., 1974, MS Thesis: "Seismic Reflection and Refraction Studies in Folded Valley and Ridge Province at Price Mountain, Montgomery County, Virginia", Virginia Polytechnic Institute and State University, Blacksburg.

Knotts, J.B. and Dunne, W.M., 1985, "Section 4", in Woodward, N.B., ed., *Valley and Ridge Thrust Belt; Balanced Structural Sections, Pennsylvania to Alabama*, University of Tennessee, pp. 16-17.

Knotts, J.B., Jr., 1984, MS Thesis: "A Structural Interpretation Across the Central Appalachians Using Gravity as an Aid", West Virginia University, Morgantown.

Kulander, B.R., and Dean, S.L., 1972, "Gravity and Structure across Browns Mountain, Wills Mountain, and Warm Springs Anticlines - Gravity Study of the Folded Plateau, West Virginia, Virginia, and Maryland", in *Appalachian Structures, Origin, Evolution, Frontiers - A Seminar*, West Virginia University and West Virginia Geological and Economic Survey, Morgantown.

Longman, I.M., 1959, "Formulas for Computing the Tidal Accelerations Due to the Moon and the Sun", in *Journal of Geophysical Research* , Vol. 64, No. 12, pp. 2351-2355.

Moses, Michael J., 1988, MS Thesis: "The Gravity Field over the Bane Dome in Giles County, Virginia", Virginia Polytechnic Institute and State University, Blacksburg.

Read,J.F., (in press), "Evolution of Cambro-Ordivician Passive Margin, Uniteds States Appalachians", in *Decade of North American Geology Synthesis Volume, Appalachian-Ouachita*

Robinson, E.S., 1974, "A Reconnaisance of Tidal Gravity in Southeastern United States", in *Journal of Geophysical Research* , Vol. 79, No. 29, pp. 4418-4424.

Robinson, E.S., and Çoruh, C., 1988, *Basic Exploration Geophysics*, John Wiley & Sons, New York.

SAS Institute, Incorporated, 1985, *SAS User's Guide*, 5 Volumes, Cary, North Carolina

Sears, C.E., and Robinson, E.S., 1971, "Relations of Bouguer Anomalies to Geological Structures in the New River District of Virginia", *Geological Society of America Bulletin*, Vol. 82, pp. 2631-2638.

Stovall, R.L., Robinson, E.S., and Bartholomew, (in press), "Gravity Anomalies and Geology in the Blue Ridge Province Near Floyd, Virginia", in *Contributions to Virginia Geology*, No. VI.

Talwani, M., Worzel, J.L., and Landisman, M., 1959, "Rapid Gravity Computations for Two-Dimensional Bodies with Application to the Mendicino Submarine Fracture Zone", *Journal of Geophysical Research*, Vol. 64, pp. 49-59.

Thomas, W.A., 1983, "Continental Margins, Orogenic Belts, and Intracratonic Structures", *Geology (Update of Appalachian Salients and Recesses)*, Vol. 11, No. 5, pp. 270-272.

Wilson, T.H., 1985, "Section 3 (right half)" and "Section 5", in Woodward, N.B., ed., *Valley and Ridge Thrust Belt; Balanced Structural Sections, Pennsylvania to Alabama*, University of Tennessee, pp. 7, 15, 18, and 19.

Woodward, N.B. (ed), 1985, *Valley and Ridge Thrust Belt; Balanced Structural Sections, Pennsylvania to Alabama*, University of Tennessee.

Wollard, G.P., 1979, "The New Gravity System - Changes in International Gravity Base Values and Anomaly Values", *Geophysics*, Vol. 44, No. 8, pp. 1352-1366.

Figures and Tables

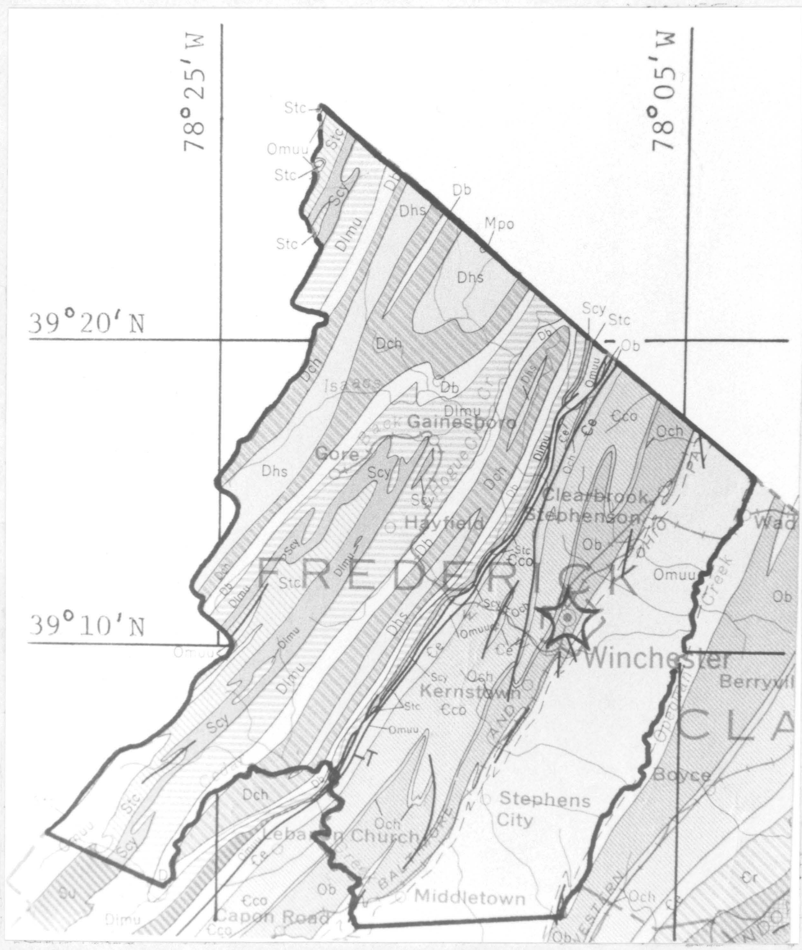

FIGURE 1. Geological map of Frederick County, Virginia (from Calver and Hobbs, 1963) showing reference latitude and longitude and geological symbols as follows: Ce = Elbrook formation; Cco = Conococheague formation; Omuu = Ordovician formations, middle and upper (Martinsburg formation); Ob = Beekmantown formation; Och = Chepultepec formation; Stc = Clinton and Tuscarora formations; Scy = Cayga group (McKenzie, Bloomsburg, Wills Creek, Tonoloway, and Keyser formations); Dlmu = Devonian formations, lower and middle (New Scotland, Helderberg, Onondaga, Marcellus, and Hamilton formations); Db = Brallier formation; Dch = Chemung formation; Dhs = Hampshire formation; Mpo = Pocono formation;

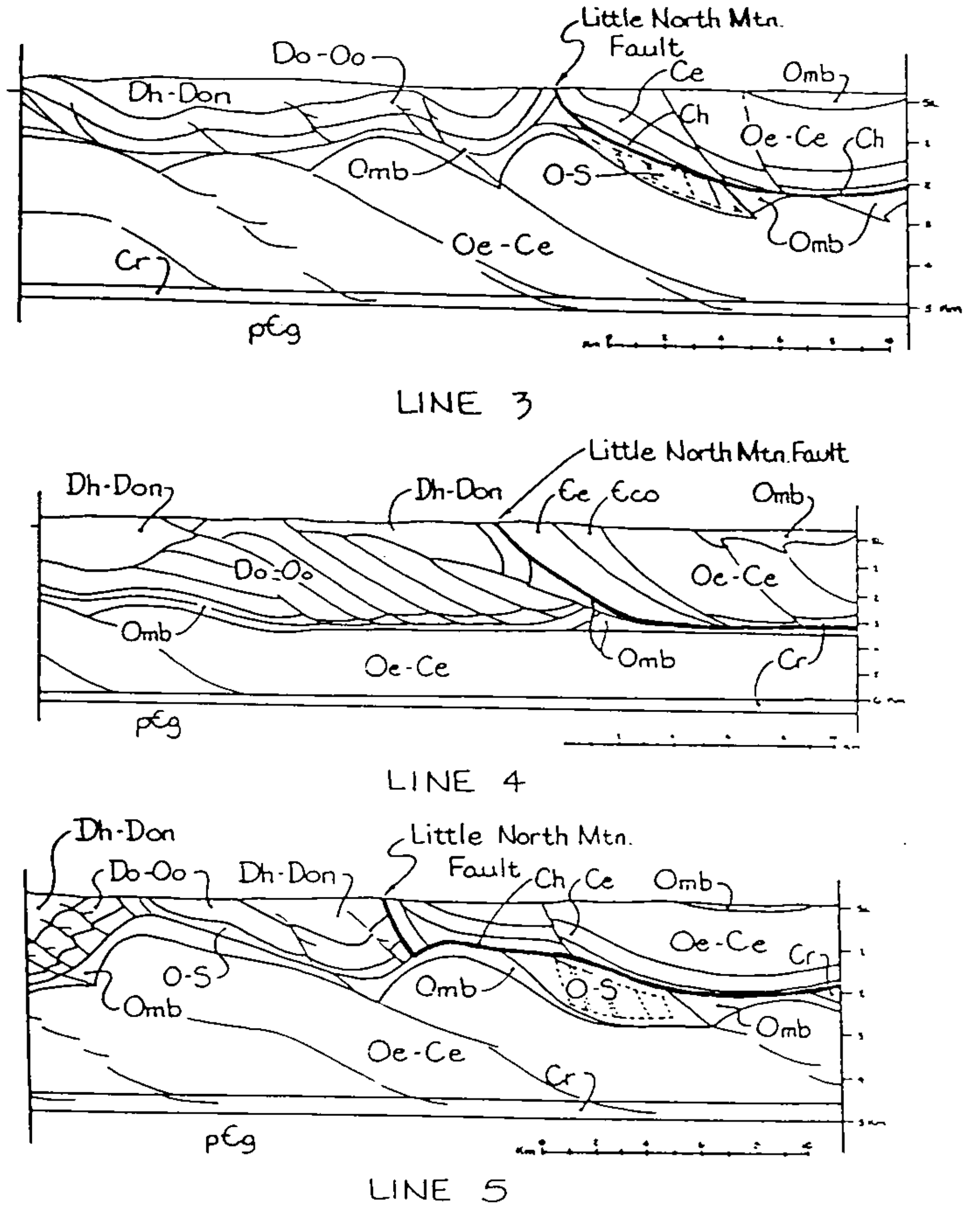

FIGURE 2. Geological cross sections through Frederick County, Virginia after Wilson, (1985) and Knotts and Dunne, (1985). See Figure 3 for locations of cross sections. The following are the symbols taken from Woodward, (1985): pCg – Precambrian crystaline basement, Grenville complex; Cr – Cambrian Rome formation; Ch – Cambrian Honaker formation (inferred); Ce – Cambrian Elbrook formation; Cco – Cambrian Conococheague formation; Oe-Ce – Cambro-Ordovician complex; Omb – Martinsburg formation; O-S – Ordovician-Silurian complex; Do-Oo – Ordovician-Devonian complex (Helderburg group); Dh-Don – Devonian complex.

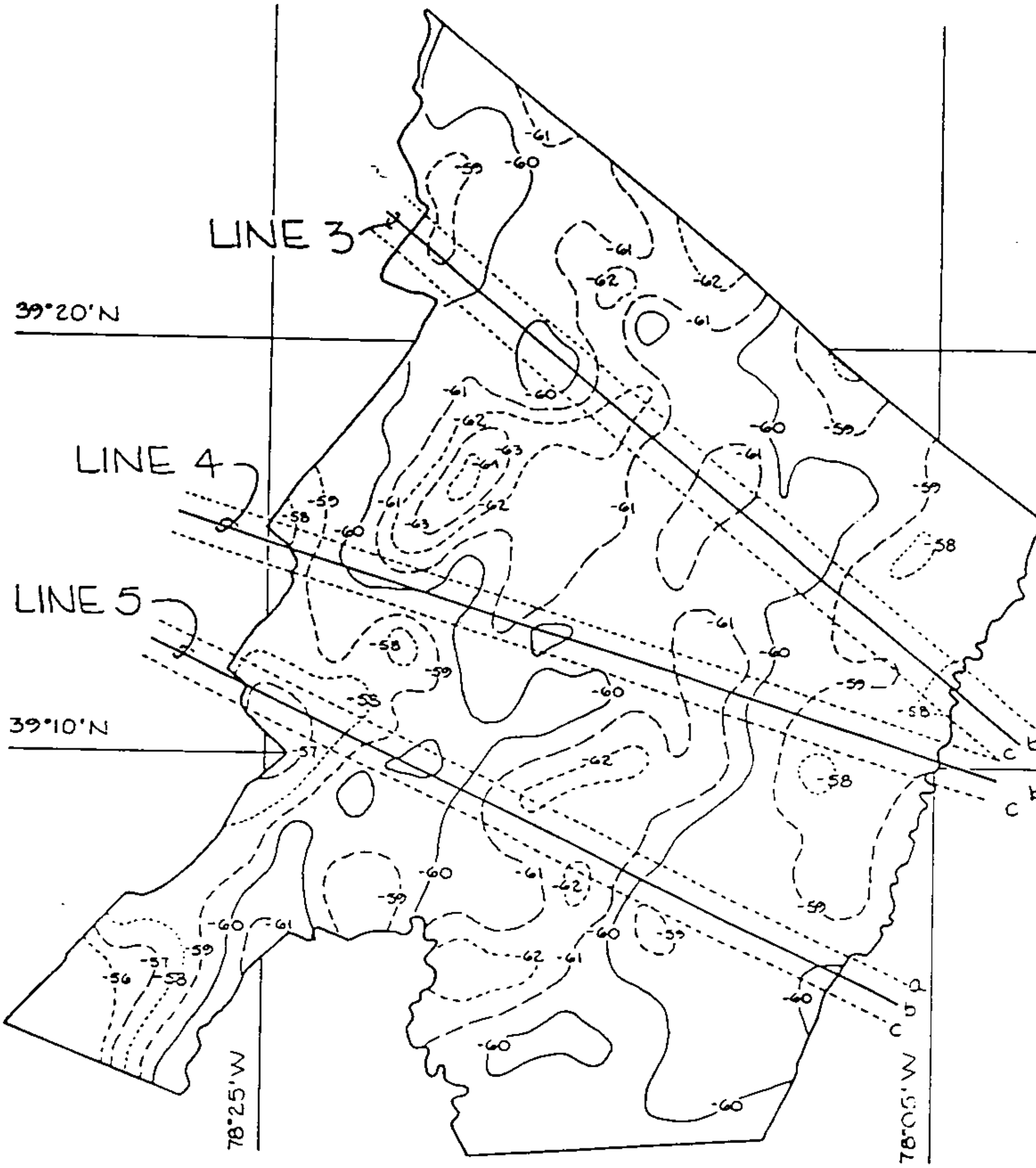

FIGURE 3 Bouguer gravity countour map of Frederick County, Virginia showing the location of the three geologic cross sections from Wilson, (1985) and Knotts and Dunne, (1985). Contour interval is 1 mgal. Lines a, b, and c are locations of Bouguer gravity profiles corresponding to each geologic cross section. Reference latitudes and longitudes are shown.

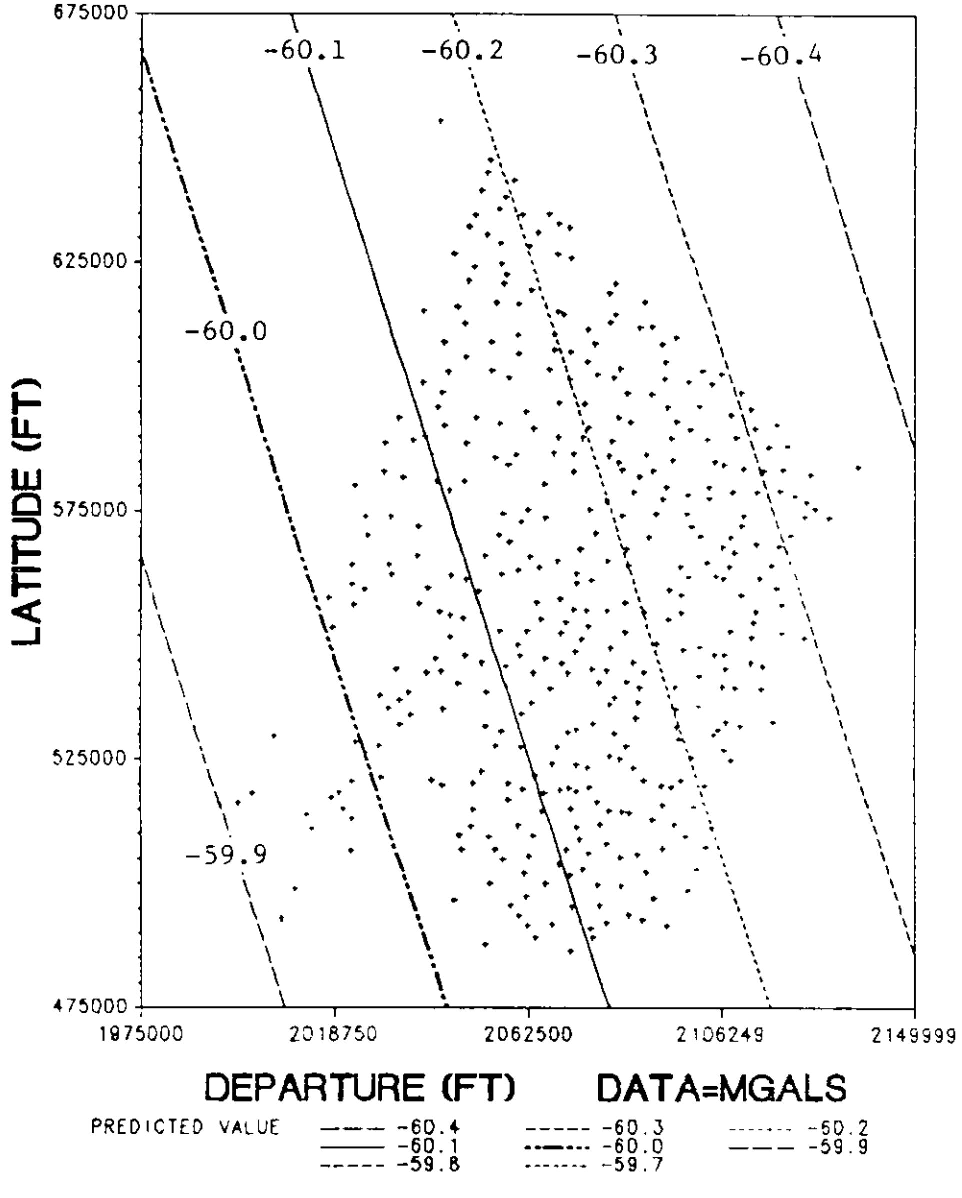

FIGURE 4a. Regional field calculated from a plane polynomial showing locations of data points. Contour interval is 0.1 mgal and dip is N65E.

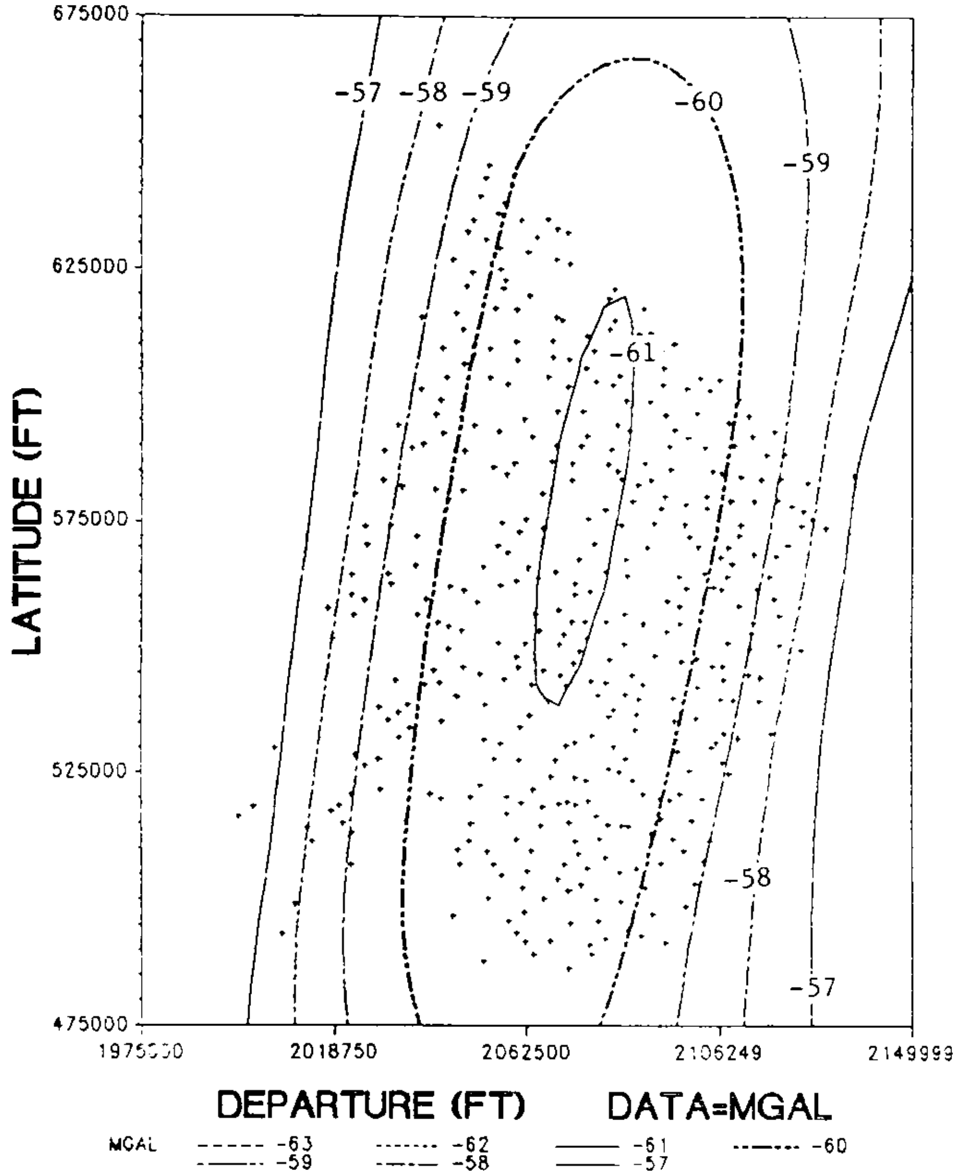

FIGURE 4b. Curve fitted to Bouguer gravity data using a quadratic polynomial and showing location of data points. Contour interval is 1 mgal and strike is N10E.

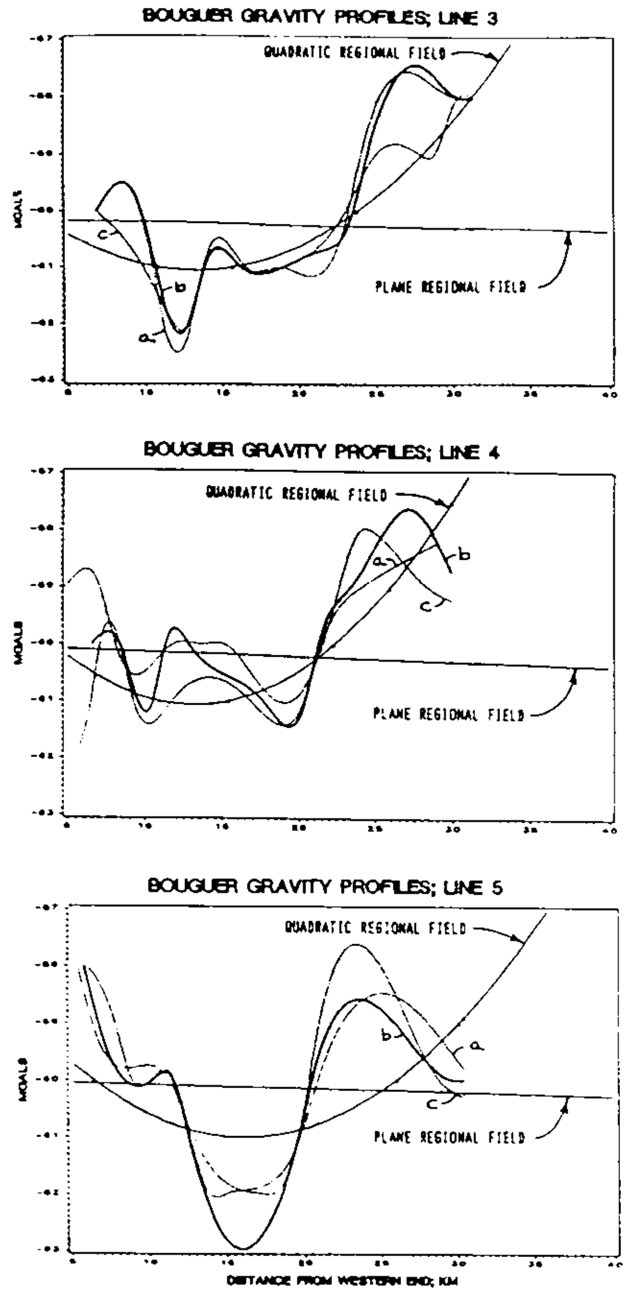

FIGURE 5. Bouguer Gravity Profiles a, b, and c for each line shown on Figure 3. Also shown, are the profiles of the plane and quadratic fields along each line.

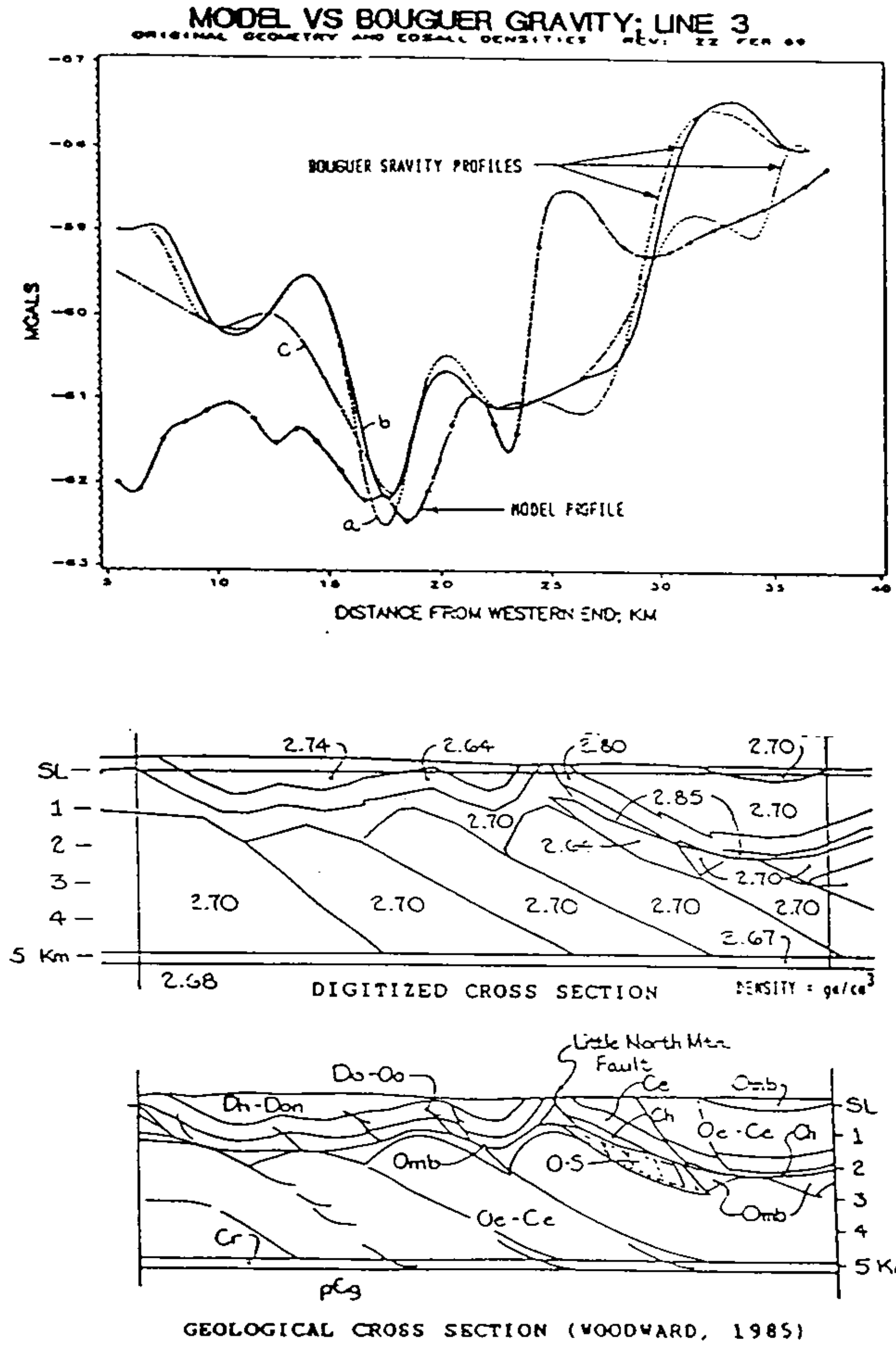

FIGURE 6. Bouguer versus Model gravity variations along Line 3 using published cross section geometry (Wilson, 1985) and densities from the literature for calculation of the model profile. Bouguer gravity profiles are calculated from field data. The deviations of profiles a, b, and c illustrate third dimension variations along strike. Densities shown on the digitized cross section are in gm/cm^3. Explanations for geologic symbols on the geological cross section are found on Figure 2 and in the text. Horizontal scale is shown on the upper figure and is the same for all figures on this page.

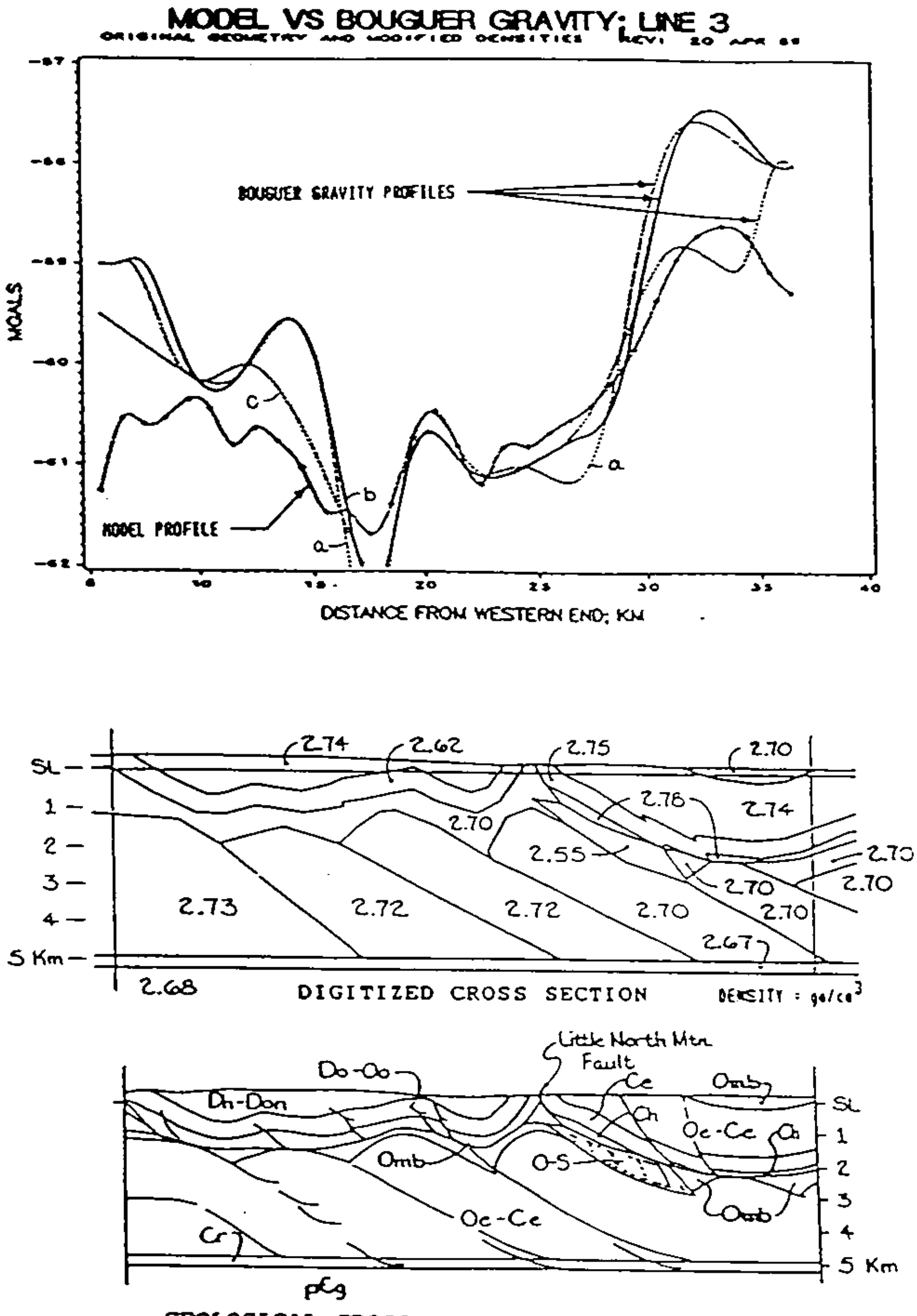

FIGURE 7. Bouguer versus Model gravity variations along Line 3 using published cross section geometry (Wilson, 1985) and densities modified as required for calculation of a model profile which agrees with the Bouguer gravity profiles. Bouguer gravity profiles are calculated from field data. The deviations of profiles a, b, and c illustrate third dimension variations along strike. Densities shown on the digitized cross section are in *gm/cm*³. Explanations for geologic symbols on the geological cross section are found on Figure 2 and in the text. Horizontal scale is shown on the upper figure and is the same for all figures on this page.

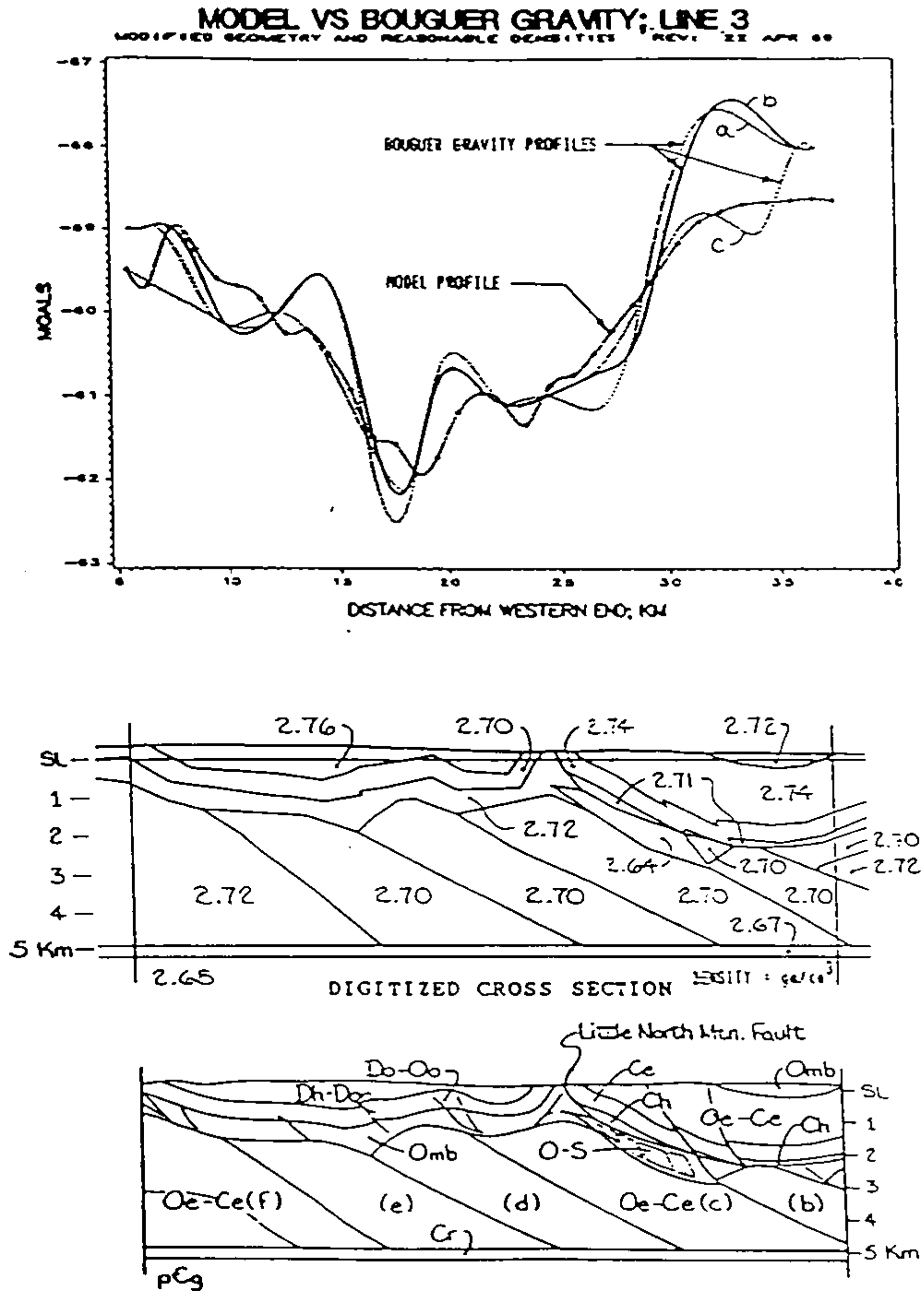

FIGURE 8. Bouguer versus Model gravity variations along Line 3 using modified cross section geometry and reasonable densities for calculation of a model profile which agrees with the Bouguer gravity profiles. Bouguer gravity profiles are calculated from field data. The deviations of profiles a, b, and c illustrate third dimension variations along strike. Densities shown on the digitized cross section are in *gm/cm*³. Explanations for geologic symbols on the geological cross section are found on Figure 2 and in the text. Horizontal scale is shown on the upper figure and is the same for all figures on this page.

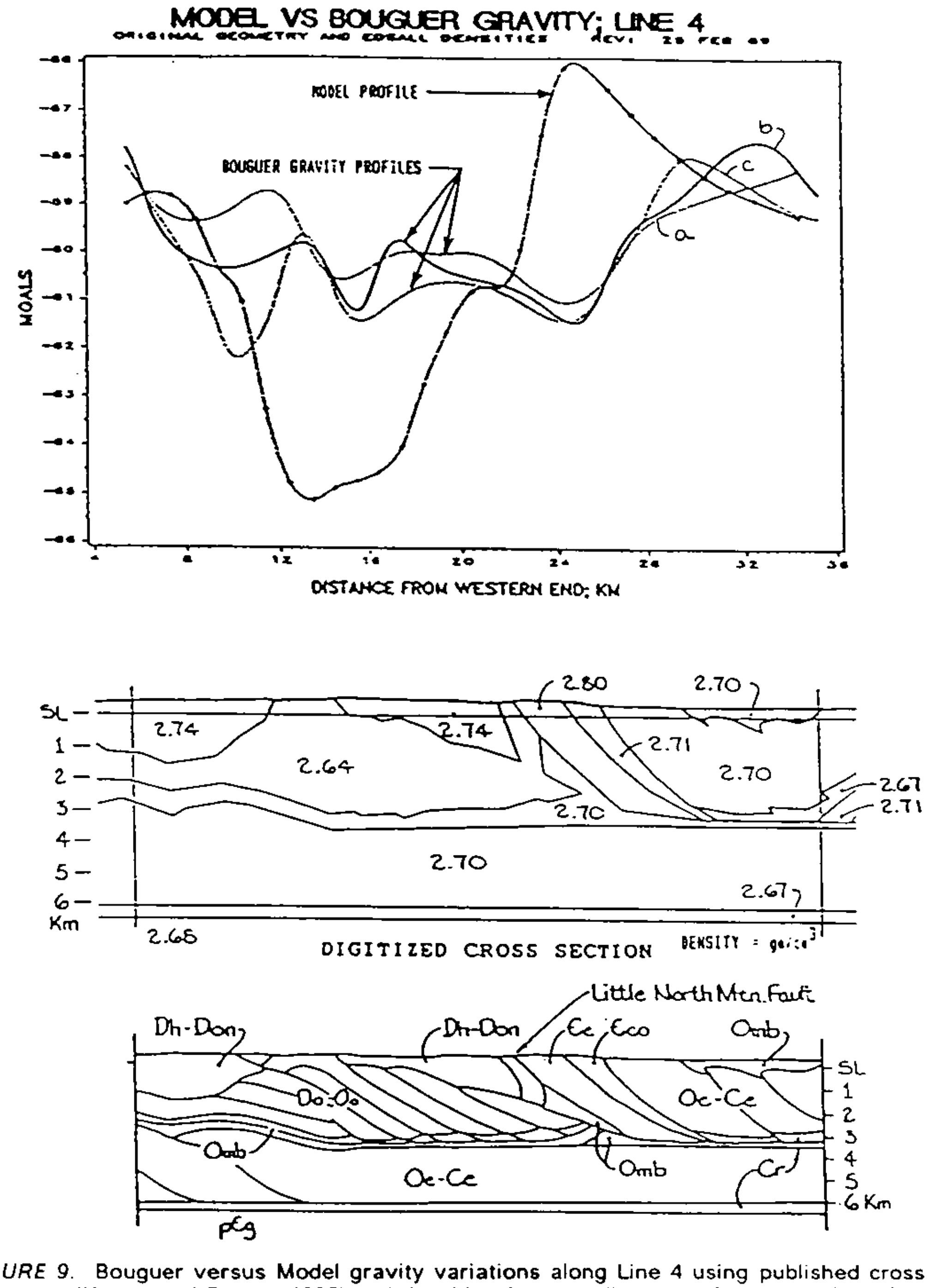

FIGURE 9. Bouguer versus Model gravity variations along Line 4 using published cross section geometry (Knotts and Dunne, 1985) and densities from the literature for calculation of the model profile. Bouguer gravity profiles are calculated from field data. The deviations of profiles a, b, and c illustrate third dimension variations along strike. Densities shown on the digitized cross section are in *gm/cm*³. Explanations for geologic symbols on the geological cross section are found on Figure 2 and in the text. Horizontal scale is shown on the upper figure and is the same for all figures on this page.

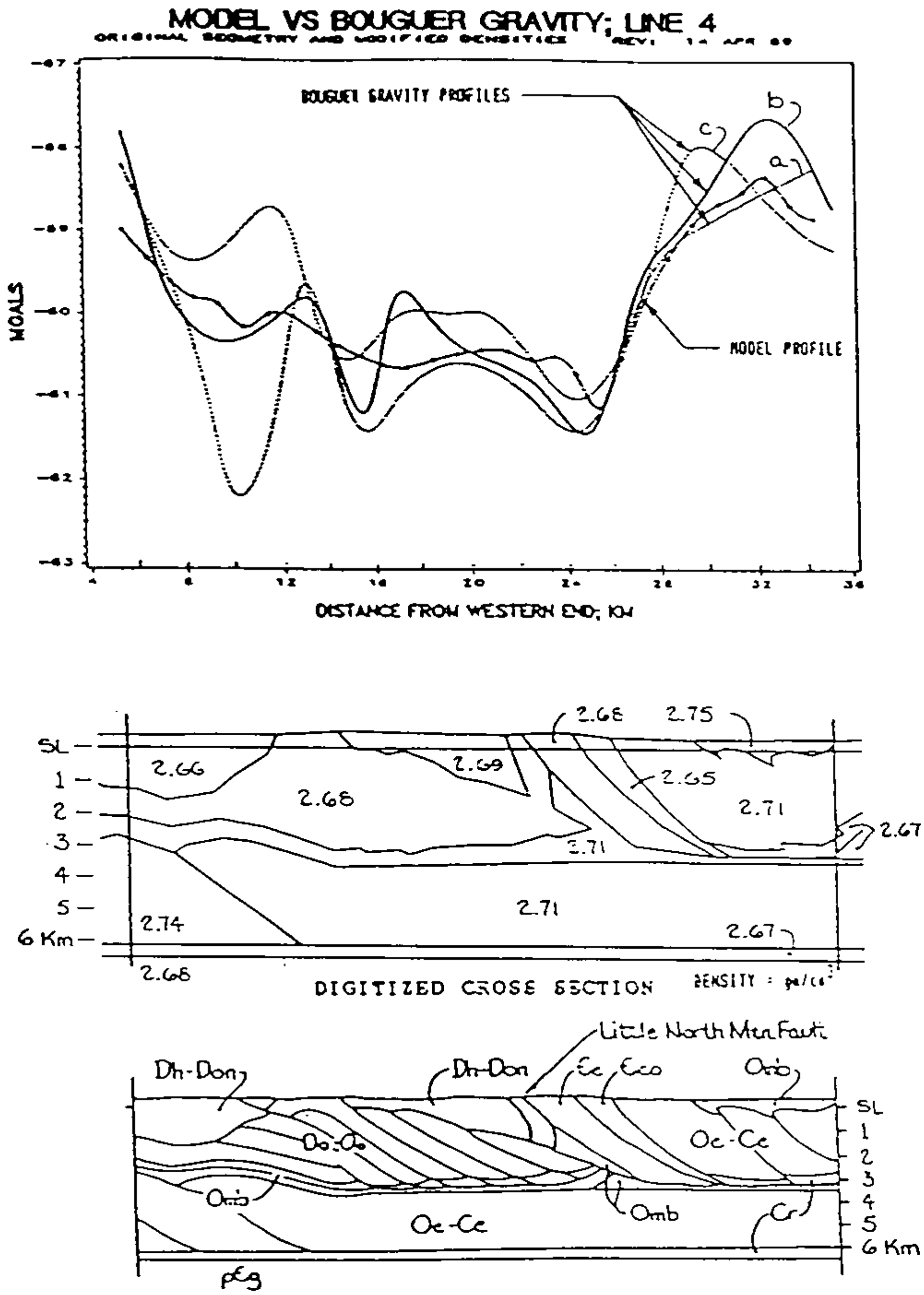

FIGURE 10. Bouguer versus Model gravity variations along Line 4 using published cross section geometry (Knotts and Dunne, 1985) and densities modified as required for calculation of a model profile which agrees with the Bouguer gravity profiles. Bouguer gravity profiles are calculated from field data. The deviations of profiles a, b, and c illustrate third dimension variations along strike. Densities shown on the digitized cross section are in *gm/cm*^{3}. Explanations for geologic symbols on the geological cross section are found on Figure 2 and in the text. Horizontal scale is shown on the upper figure and is the same for all figures on this page.

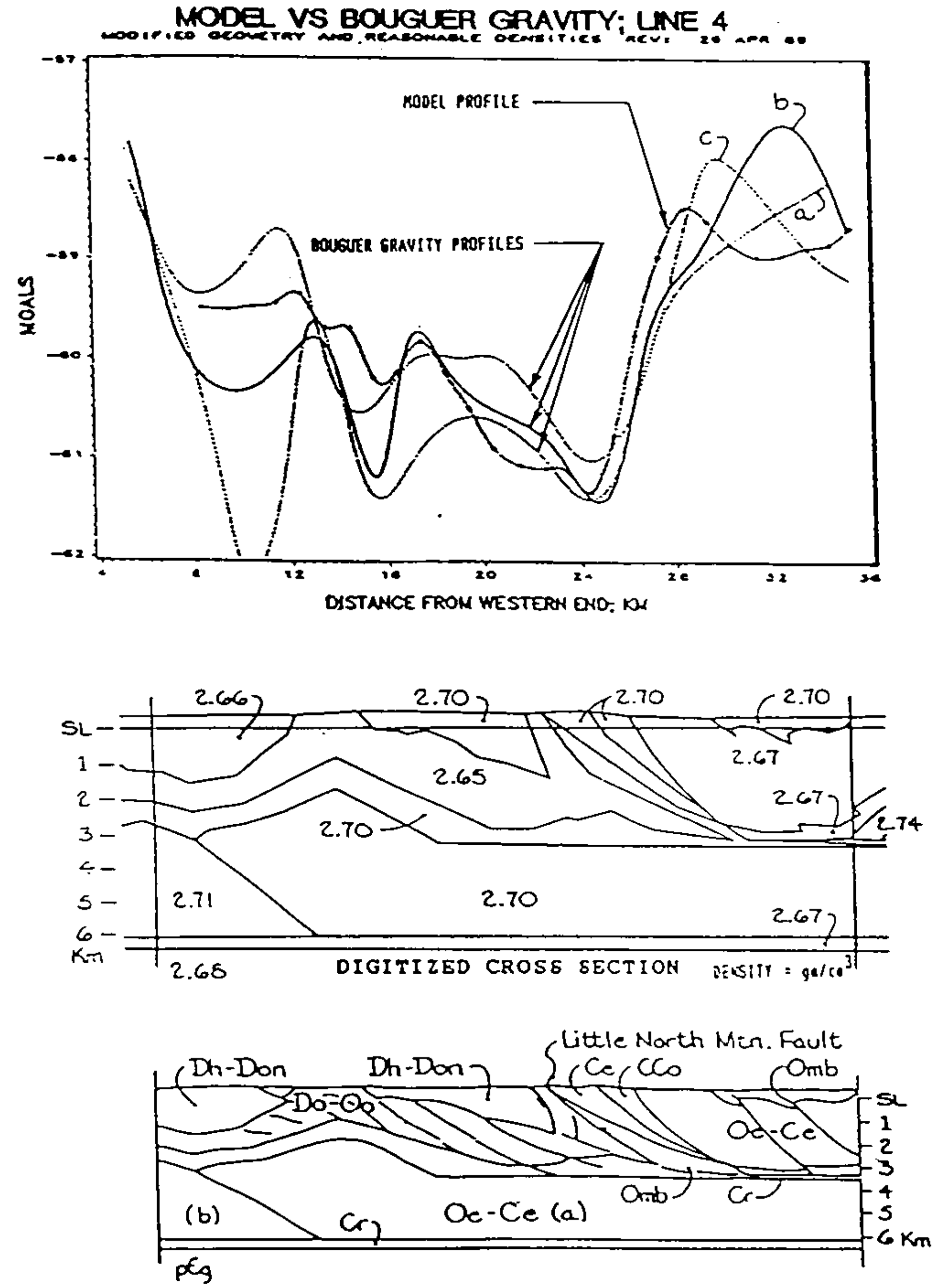

FIGURE 11. Bouguer versus Model gravity variations along Line 4 using modified cross section geometry and reasonable densities from the literature for calculation of a model profile which agrees with the Bouguer gravity profiles. Bouguer gravity profiles are calculated from field data. The deviations of profiles a, b, and c illustrate third dimension variations along strike. Densities shown on the digitized cross section are in *gm/cm*^{3}. Explanations for geologic symbols on the geological cross section are found on Figure 2 and in the text. Horizontal scale is shown on the upper figure and is the same for all figures on this page.

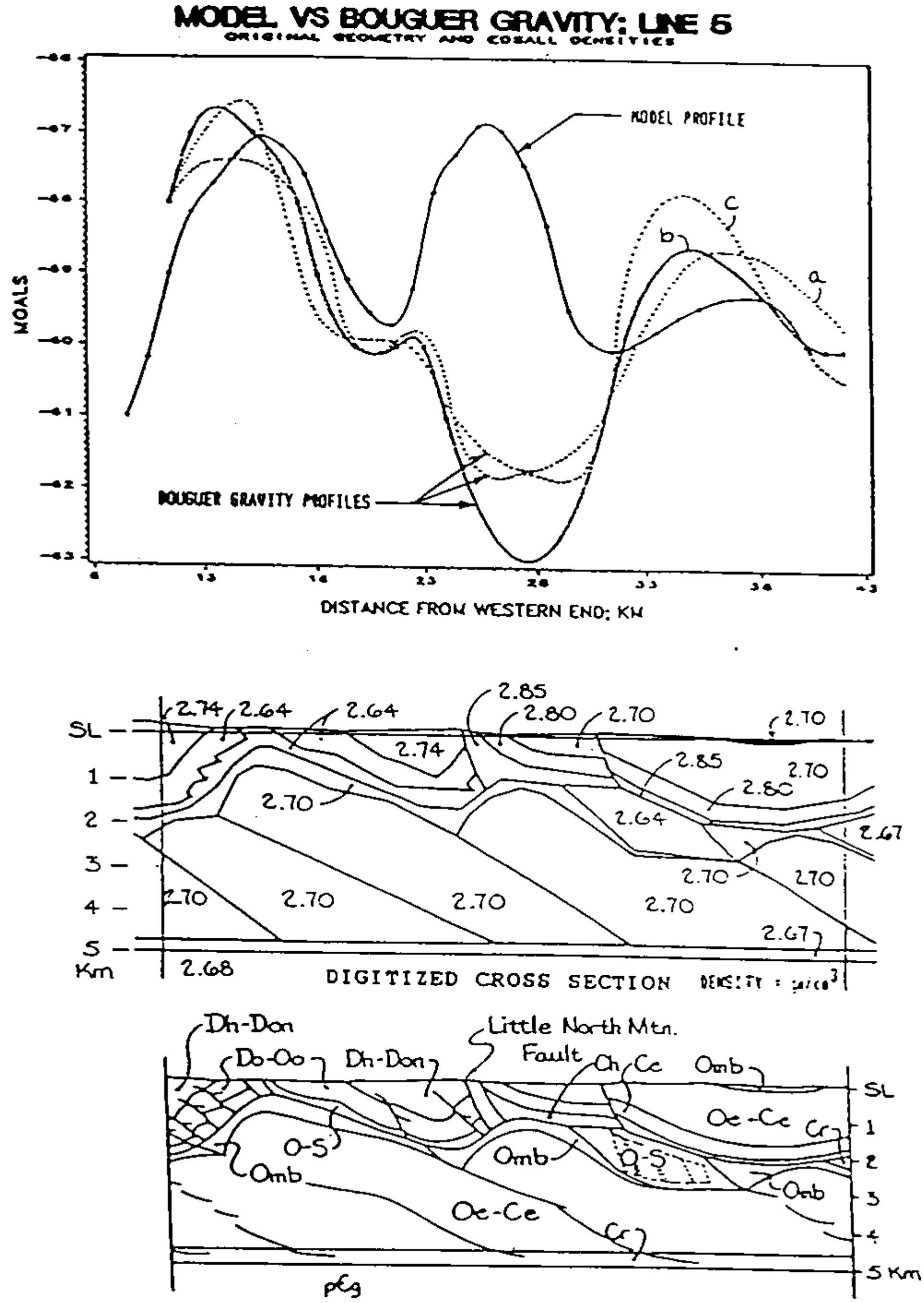

FIGURE 12. Bouguer versus Model gravity variations along Line 5 using published cross section geometry (Wilson, 1985) and densities from the literature for calculation of the model profile. Bouguer gravity profiles are calculated from field data. The deviations of profiles a, b, and c illustrate third dimension variations along strike. Densities shown on the digitized cross section are in *gm/cm*[3]. Explanations for geologic symbols on the geological cross section are found on Figure 2 and in the text. Horizontal scale is shown on the upper figure and is the same for all figures on this page.

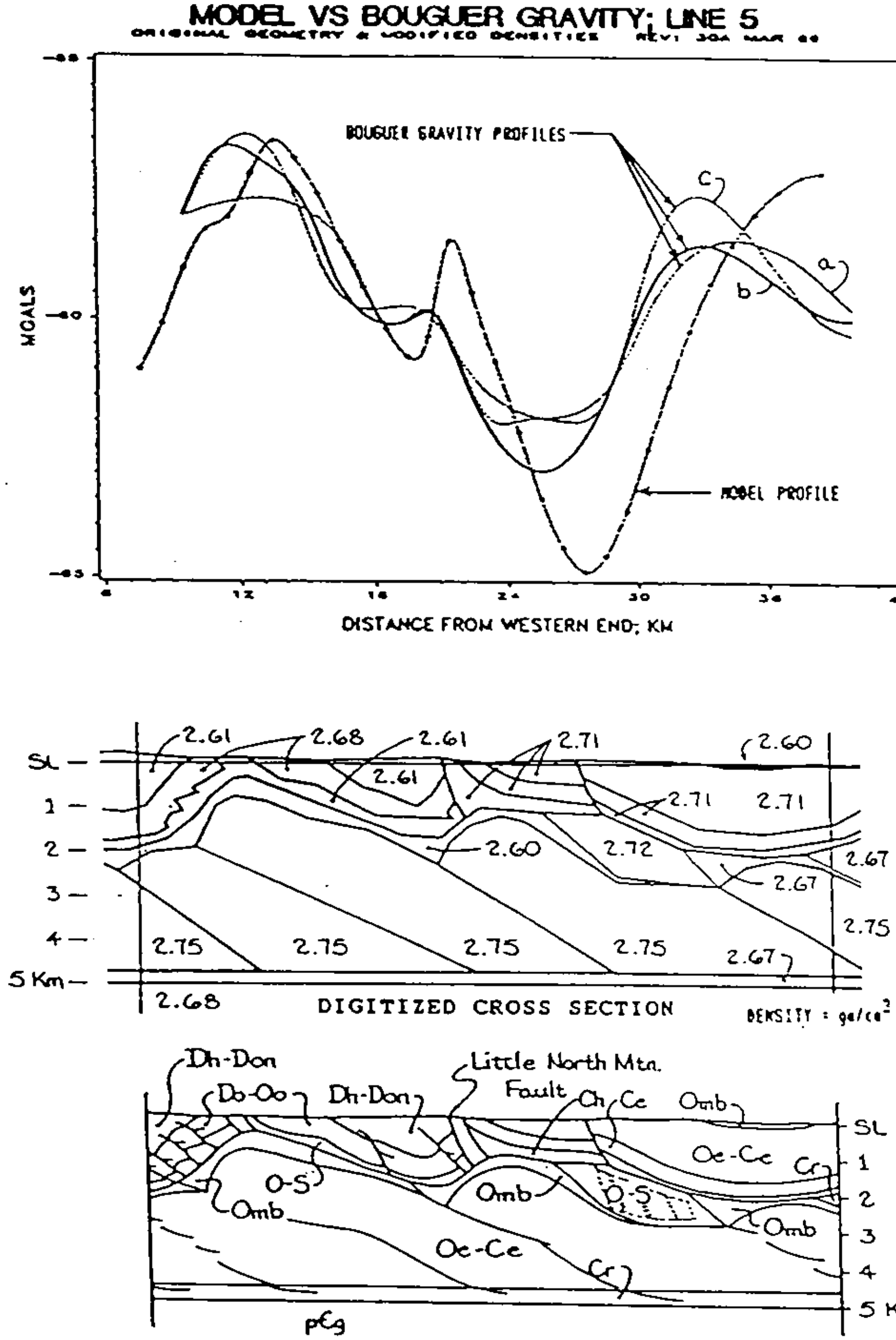

FIGURE 13. Bouguer versus Model gravity variations along Line 5 using published cross section geometry (Wilson, 1985) and densities modified as required for for calculation of a model profile which agrees with the Bouguer gravity profiles. Bouguer gravity profiles are calculated from field data. The deviations of profiles a, b, and c illustrate third dimension variations along strike. Densities shown on the digitized cross section are in *gm/cm*³. Explanations for geologic symbols on the geological cross section are found on Figure 2 and in the text. Horizontal scale is shown on the upper figure and is the same for all figures on this page.

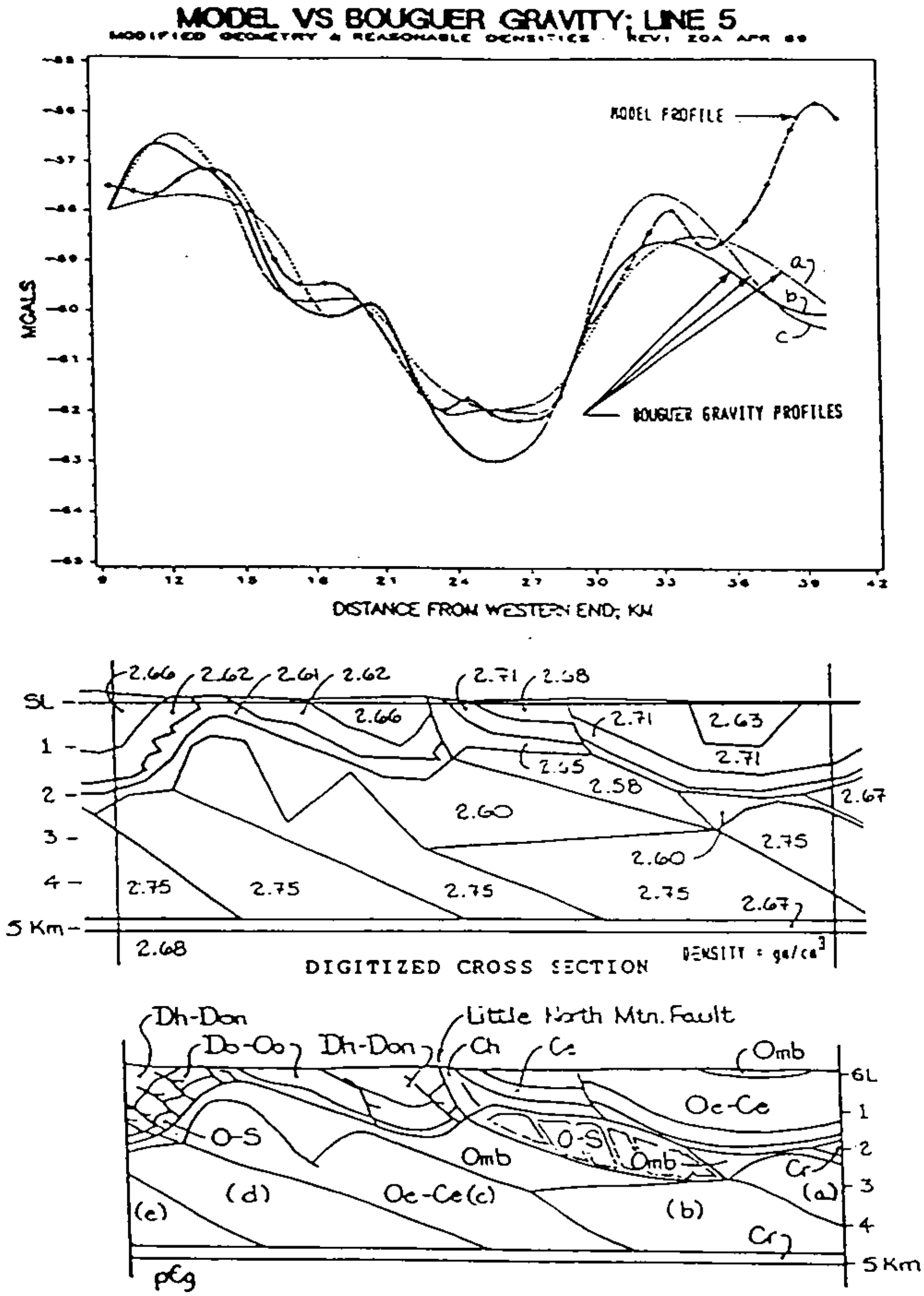

FIGURE 14. Bouguer versus Model gravity variations along Line 5 using modified cross section geometry and reasonable densities from the literature for calculation of a model profile which agrees with the Bouguer gravity profiles. Bouguer gravity profiles are calculated from field data. The deviations of profiles a, b, and c illustrate third dimension variations along strike. Densities shown on the digitized cross section are in *gm/cm*³. Explanations for geologic symbols on the geological cross section are found on Figure 2 and in the text. Horizontal scale is shown on the upper figure and is the same for all figures on this page.

TABLE 1.

Density values for sedimentary rocks in the southern Appalachians (Edsall, 1974 and Kolich, 1974).

Age	Formation	Density	Age	Formation	Density
Mississippian	Price sandstone	2.67		Kingsport dolomite	2.79
	post-Cloyd claystone	2.72		Longview limestone	2.71
	Cloyd conglomerate	2.58		Chepultepec limestone	2.72
	Parrott sandstone	2.62		Chepultepec dolomite	2.83
Devonian	Chemung sandstone	2.61	Cambrian	Copper Ridge sandstone	2.71
	Millboro shale	2.74		Copper Ridge dolomite	2.81
Silurian	Keefer sandstone	2.64		Elbrook dolomite	2.80
	Rose Hill sandstone	3.07		Honaker dolomite	2.85
	Tuscarora sandstone	2.64		Rome shale	2.67
Ordovician	Juniata sandstone	2.62		Rome dolomite	2.83
	Martinsburg shale	2.70		Shady dolomite	2.84
	Eggleston conglomerate	2.65		Shady limestone	2.73
	Moccasin shale	2.71		Erwin sandstone	2.59
	Bays sandstone	2.68		Hampton shale	2.71
	Witten limestone	2.68		Unicoi sandstone	2.67
	Liberty Hall shale	2.69	Precambrian	Augen gneiss	2.70
	Lincolnshire limestone	2.70		Amphibolite	3.00
				Lynchburg amphibolite	2.97
	Five Oaks limestone	2.70		Lynchburg gneiss	2.64
	New Market limestone	2.72		Grenville gneiss	2.66
	Elway limestone	2.68			
	Upper Knox dolomite	2.82			

TABLE 2
Model density values for Line 3

19 bodies
(gm/cm^3)

	from literature	required for fit	reasonable
Omb	2.70[e]	2.70	2.72[d]
Dh-Don	2.74[e]	2.74	2.76[e]
Do-Oo	2.64[e]	2.62	2.70[e]
Oe-Cco	2.70[■]	2.74	2.74[■]
Ce	2.80[e]	2.75	2.74[■]
Ch	2.85[e]	2.78	2.71[by]
Omb	2.70[e]	2.70	2.72[d]
Omb	2.70[e]	2.70	2.70[e]
Omb	2.70[e]	2.70	2.70[e]
Cr	2.67[e]	2.57	2.67[e]
O-S	2.64[■]	2.55	2.64[■]
Oe-Ce(a)	2.70[■]	2.70	2.72[■]
Oe-Ce(b)	2.70[■]	2.70	2.72[■]
Oe-Ce(c)	2.70[■]	2.70	2.70[■]
Oe-Ce(d)	2.70[■]	2.72	2.70[■]
Oe-Ce(e)	2.70[■]	2.72	2.70[■]
Oe-Ce(f)	2.70[■]	2.73	2.72[■]
Cr	2.67[e]	2.57	2.67[e]
pCg	2.68[kn]	2.58	2.68[kn]

Sources:
- [d] - Dean, (1966)
- [e] - Edsall, (1974) and Kolich, (1974)
- [by] - Byerly, (1973)
- [k] - Kulander and Dean, (1972)
- [kn] - Knotts, (1984)
- [■] - composite estimate based on Edsall, (1974) and Kolich, (1974)

TABLE 3
Model density values for Line 4

15 bodies
(gm/cm^3)

	from literature	required for fit	reasonable
Dh-Don	2.74[e]	2.66	2.66[by]
Dh-Don	2.74[e]	2.69	2.70[m]
Do-Do	2.64[e]	2.68	2.65[e]
Omb	2.70[e]	2.75	2.70[e]
CCo	2.71[e]	2.65	2.70[e]
Ce	2.80[e]	2.68	2.70[kn]
Oe-Ce	2.70[m]	2.71	2.67[kn]
Cr	2.67[e]	2.67	2.67[e]
CpCc	2.71[m]	2.67	2.74[m]
pCg	2.68[kn]	2.68	2.68[kn]
Cmb	2.70[e]	2.71	2.70[e]
Oe-Ce(a)	2.70[m]	2.71	2.70[kn]
Oe-Ce(b)	2.70[m]	2.74	2.71[kn]
Cr	2.67[e]	2.67	2.67[e]
pCg	2.68[kn]	2.68	2.68[kn]

Sources: [e] - Edsall, (1974) and Kolich, (1974)
[by] - Byerly, (1973)
[k] - Kulander and Dean, (1972)
[kn] - Knotts, (1984)
[m] - composite estimate based on Edsall, (1974) and Kolich, (1974)

TABLE 4
Model density values for Line 5

26 bodies
(gm/cm^3)

	from literature	required for fit	reasonable
Dh-Don	2.74[e]	2.61	2.66
Dh-Don	2.74[e]	2.61	2.66
Omb	2.70[e]	2.60	2.63
Oe-Ce	2.70[m]	2.71	2.71
Oe-Ce	2.70[m]	2.71	2.68
Ce	2.80[e]	2.71	2.71[kn]
Ce	2.80[e]	2.71	2.71[kn]
Ch	2.85[e]	2.71	Omb 2.65[kn]
Ch	2.85[e]	2.71	Omb 2.65[kn]
Do-Oo	2.64[e]	2.68	2.62
Do-Oo	2.64[e]	2.68	2.62
O-S	2.64[m]	2.61	2.61
Cr	2.67[e]	2.67	2.67
CpCc	2.71[m]	2.71	2.60[m]
pCg	2.68[kn]	2.68	2.68
Cr	2.67[e]	2.67	2.67
Omb	2.70[e]	2.60	2.60[kn]
O-S	2.64[m]	2.72	2.58[m]
Omb	2.70[e]	2.60	2.60[kn]
Oe-Ce(e)	2.70[m]	2.75	2.75
Oe-Ce(d)	2.70[m]	2.75	2.75
Oe-Ce(c)	2.70[m]	2.75	2.75
Oe-Ce(b)	2.70[m]	2.75	2.75
Oe-Ce(a)	2.70[m]	2.75	2.75
Cr	2.67[e]	2.67	2.67
pCg	2.68[kn]	2.68	2.68

Sources: e - Edsall, (1974) and Kolich, (1974)
by - Byerly, (1973)
k - Kulander and Dean, (1972)
kn - Knotts, (1984)
m - composite estimate based on Edsall, (1974) and Kolich, (1974)

Appendix A. Bouguer Gravity Data Set

STA = Station number; format = ddnnn
    dd + 150 = 1988 Julian date of reading
    nnn = reading number
    dd000 = morning base station
    dd999 = evening base station
XPLOT = X state grid coordinate, in feet, of the station
YPLOT = Y state grid coordinate, in feet, of the station
ELEV = Station elevation in feet above mean sea level
FA = Free air gravity in milligals
SBG = Simple Bouguer Gravity in milligals
CBG = Complete Bouguer Gravity in milligals
TC = Terrain Correction

STA	XPLOT	YPLOT	ELEV	FA	SBG	CBG	TC
8000	2092115.	548871.	745.	-38.1	-61.9	-61.7	0.185
8001	2089073.	543069.	756.	-37.8	-62.0	-61.8	0.157
8002	2088260.	540043.	775.	-35.9	-60.6	-60.6	0.031
8003	2087704.	536945.	746.	-36.5	-60.3	-59.9	0.359
8004	2087288.	533884.	756.	-34.8	-58.9	-58.8	0.095
8005	2085109.	541162.	810.	-36.3	-62.2	-61.7	0.462
8006	2082509.	538021.	813.	-35.7	-61.6	-61.6	0.059
8007	2081323.	536633.	850.	-34.7	-61.9	-61.3	0.665
8008	2077505.	532761.	759.	-38.0	-62.3	-61.9	0.377
8009	2073707.	531475.	809.	-36.4	-62.3	-61.6	0.673
8010	2078814.	540887.	792.	-36.1	-61.5	-60.7	0.763
8011	2077387.	543796.	823.	-37.3	-63.6	-63.5	0.084
8012	2071831.	542906.	828.	-35.0	-61.5	-60.7	0.727
8013	2080763.	543406.	812.	-35.7	-61.6	-61.6	0.044
8014	2086627.	544991.	797.	-35.9	-61.4	-60.9	0.515
8999	2092115.	548871.	745.	-38.1	-61.9	-61.7	0.185
9000	2092115.	548871.	745.	-38.1	-61.9	-61.7	0.185
9001	2081627.	548071.	835.	-35.0	-61.7	-61.6	0.035
9002	2084963.	551141.	782.	-36.0	-61.0	-60.6	0.412
9003	2089031.	555198.	780.	-36.6	-61.5	-61.5	0.053
9004	2084886.	557151.	874.	-33.1	-61.0	-61.0	0.075
9005	2080640.	555498.	851.	-33.7	-60.9	-60.6	0.283
9006	2075906.	555520.	897.	-32.5	-61.2	-61.1	0.107
9007	2073043.	555658.	841.	-34.7	-61.6	-56.8	4.758
9008	2071406.	553067.	907.	-32.3	-61.3	-58.2	3.158
9009	2073736.	561087.	899.	-31.9	-60.7	-60.4	0.275
9010	2073787.	563090.	952.	-30.5	-61.0	-60.8	0.156
9011	2074595.	567937.	885.	-32.4	-60.7	-60.5	0.195
9012	2077929.	571042.	957.	-30.0	-60.6	-60.4	0.213
9013	2076697.	575883.	898.	-32.0	-60.7	-60.5	0.170
9014	2080722.	565515.	865.	-32.7	-60.4	-60.0	0.315
9015	2077192.	561607.	944.	-30.3	-60.5	-59.9	0.637
9016	2085542.	564583.	897.	-32.7	-61.4	-61.3	0.111
9017	2085021.	567932.	900.	-32.2	-61.0	-60.9	0.064
9018	2084235.	574632.	896.	-32.8	-61.5	-61.4	0.147
9019	2090141.	570244.	902.	-32.0	-60.8	-60.7	0.076
9020	2091739.	575058.	921.	-30.9	-60.4	-59.8	0.617
9999	2092115.	548871.	745.	-38.1	-61.9	-61.7	0.185
15000	2092115.	548871.	745.	-38.1	-61.9	-61.7	0.185
15001	2098679.	574937.	765.	-37.2	-61.6	-61.3	0.313
15002	2099821.	572356.	731.	-37.1	-60.5	-59.9	0.635
15003	2101812.	570469.	726.	-37.3	-60.5	-60.5	0.024
15004	2097415.	564443.	716.	-37.5	-60.4	-59.9	0.457
15005	2103193.	565084.	702.	-37.0	-59.5	-59.5	0.016
15006	2105244.	562397.	684.	-37.7	-59.5	-59.5	0.015

STA	XPLOT	YPLOT	ELEV	FA	SBG	CBG	TC
15007	2099180.	562155.	696.	-38.0	-60.3	-59.9	0.387
15008	2097521.	558725.	725.	-36.9	-60.1	-60.0	0.113
15009	2094911.	559662.	747.	-37.6	-61.5	-61.4	0.135
15010	2094592.	553651.	712.	-37.9	-60.7	-59.9	0.806
15011	2097478.	555119.	736.	-36.2	-59.7	-59.7	0.023
15012	2098102.	547654.	726.	-36.1	-59.4	-59.3	0.054
15013	2101530.	548250.	636.	-39.0	-59.3	-58.8	0.561
15014	2104995.	546698.	686.	-37.4	-59.3	-59.3	0.063
15015	2101525.	542386.	665.	-37.7	-59.0	-58.7	0.308
15016	2096201.	540217.	733.	-35.7	-59.2	-59.1	0.041
15017	2101350.	536157.	712.	-36.7	-59.4	-59.4	0.022
15018	2105880.	531477.	595.	-40.4	-59.4	-58.6	0.859
15019	2096445.	535592.	726.	-36.0	-59.2	-59.2	0.015
15020	2096770.	532060.	723.	-36.1	-59.2	-59.2	0.010
15999	2092115.	548871.	745.	-38.1	-61.9	-61.7	0.185
16000	2092115.	548871.	745.	-38.1	-61.9	-61.7	0.185
16001	2076369.	552280.	913.	-32.2	-61.4	-61.3	0.068
16002	2074931.	549799.	897.	-32.7	-61.4	-61.3	0.061
16003	2073464.	547172.	873.	-33.8	-61.7	-61.6	0.066
16004	2107117.	527330.	601.	-40.2	-59.4	-59.2	0.254
16005	2108799.	525297.	670.	-37.4	-58.8	-58.8	0.014
16999	2092115.	548871.	745.	-38.1	-61.9	-61.7	0.185
17000	2092115.	548871.	745.	-38.1	-61.9	-61.7	0.185
17001	2081191.	515144.	754.	-35.1	-59.2	-59.1	0.051
17002	2084144.	515044.	769.	-34.7	-59.3	-59.2	0.104
17003	2085848.	514831.	752.	-35.3	-59.4	-59.1	0.270
17004	2091076.	513428.	738.	-36.1	-59.7	-59.7	0.013
17005	2093283.	507499.	686.	-37.3	-59.3	-59.2	0.038
17006	2096105.	512317.	708.	-36.9	-59.5	-59.5	0.012
17007	2098386.	509995.	713.	-36.5	-59.3	-59.2	0.080
17008	2102880.	507827.	672.	-37.9	-59.4	-59.3	0.055
17009	2100825.	503339.	691.	-37.5	-59.6	-59.4	0.188
17010	2098967.	499034.	665.	-38.9	-60.2	-60.0	0.126
17011	2094192.	491878.	548.	-43.4	-60.9	-60.7	0.227
17012	2091246.	497367.	676.	-38.2	-59.8	-59.8	0.025
17013	2089665.	502643.	694.	-37.3	-59.5	-59.5	0.061
17014	2087494.	506314.	737.	-36.3	-59.9	-59.8	0.025
17015	2083805.	505683.	661.	-39.2	-60.3	-60.2	0.157
17016	2084051.	499892.	714.	-37.0	-59.8	-59.7	0.084
17017	2085461.	494142.	700.	-37.7	-60.1	-59.8	0.291
17018	2088732.	493170.	670.	-38.6	-60.0	-59.9	0.124
17999	2092115.	548871.	745.	-38.1	-61.9	-61.7	0.185
18000	2092115.	548871.	745.	-38.1	-61.9	-61.7	0.185
18001	2072270.	486746.	695.	-38.6	-60.8	-60.1	0.692
18002	2077235.	489564.	664.	-39.7	-61.0	-60.9	0.040

STA	XPLOT	YPLOT	ELEV	FA	SBG	CBG	TC
18003	2080381.	492524.	677.	-39.4	-61.0	-60.9	0.159
18004	2078864.	496016.	701.	-37.5	-59.9	-59.9	0.041
18005	2078425.	500239.	671.	-39.2	-60.7	-60.6	0.039
18006	2076532.	506498.	734.	-36.1	-59.6	-59.6	0.016
18007	2075207.	503289.	734.	-36.1	-59.6	-59.6	0.049
18008	2072143.	502078.	727.	-37.0	-60.2	-60.2	0.015
18009	2072700.	495670.	658.	-39.3	-60.3	-60.3	0.018
18010	2071362.	507212.	737.	-35.6	-59.2	-59.2	0.023
18011	2074394.	509442.	784.	-35.6	-60.7	-60.6	0.066
18012	2073876.	511808.	747.	-36.9	-60.8	-60.7	0.064
18013	2072361.	515519.	810.	-34.8	-60.7	-60.6	0.071
18014	2073770.	519128.	762.	-36.4	-60.8	-60.6	0.172
18015	2072037.	519670.	795.	-36.6	-62.0	-62.0	0.047
18016	2078546.	516884.	714.	-37.5	-60.3	-59.9	0.401
18017	2079184.	512370.	753.	-36.2	-60.3	-60.2	0.026
18018	2080360.	508513.	732.	-37.9	-61.3	-61.3	0.012
18019	2093280.	516277.	724.	-37.0	-60.2	-60.2	0.010
18020	2095311.	519927.	724.	-36.8	-59.9	-59.9	0.015
18021	2097662.	521210.	686.	-37.7	-59.7	-59.5	0.143
18022	2102661.	520282.	697.	-36.8	-59.1	-59.1	0.020
18023	2104227.	511875.	677.	-39.0	-60.7	-60.6	0.040
18024	2100152.	515902.	695.	-37.2	-59.4	-59.4	0.046
18999	2092115.	548871.	745.	-38.1	-61.9	-61.7	0.185
22000	2092115.	548871.	745.	-38.1	-61.9	-61.7	0.185
22001	2104664.	530488.	690.	-36.7	-58.7	-58.7	0.010
22002	2099745.	525843.	695.	-36.9	-59.1	-59.0	0.092
22003	2097035.	529585.	705.	-36.7	-59.3	-59.3	0.021
22004	2093210.	520210.	734.	-36.3	-59.8	-59.8	0.003
22005	2089119.	521252.	729.	-36.1	-59.4	-59.4	0.077
22006	2086584.	523793.	737.	-36.2	-59.8	-59.6	0.183
22007	2083741.	525569.	698.	-36.8	-59.2	-59.0	0.131
22008	2085180.	528050.	740.	-36.1	-59.7	-59.7	0.020
22009	2081327.	526217.	730.	-35.5	-58.8	-58.6	0.162
22010	2082363.	530663.	793.	-34.6	-60.0	-59.8	0.131
22011	2076282.	523907.	781.	-35.9	-60.9	-60.6	0.258
22012	2073670.	524373.	827.	-35.5	-61.9	-61.8	0.067
22013	2076720.	519902.	760.	-35.2	-59.5	-59.2	0.258
22014	2069779.	504294.	764.	-35.8	-60.3	-60.1	0.159
22015	2066580.	500425.	720.	-37.4	-60.4	-60.3	0.110
22016	2060432.	493817.	714.	-37.4	-60.2	-60.1	0.116
22017	2076974.	491384.	717.	-37.4	-60.4	-60.3	0.084
22018	2053028.	488083.	561.	-42.9	-60.9	-60.8	0.097
22019	2046192.	496993.	746.	-37.5	-61.4	-61.2	0.132
22020	2047764.	507267.	772.	-36.9	-61.6	-61.2	0.433
22021	2047190.	510216.	722.	-38.7	-61.8	-61.7	0.068

STA	XPLOT	YPLOT	ELEV	FA	SBG	CBG	TC
22022	2049998.	511933.	735.	-38.8	-62.3	-62.1	0.201
22023	2054063.	509792.	798.	-36.6	-62.1	-62.0	0.128
22024	2055403.	507246.	714.	-37.7	-60.5	-60.4	0.072
22025	2057139.	505210.	689.	-38.3	-60.3	-60.3	0.044
22026	2062269.	497865.	662.	-39.2	-60.3	-60.3	0.026
22027	2058608.	495962.	660.	-39.1	-60.2	-59.9	0.308
22028	2054224.	500469.	649.	-40.3	-61.0	-60.8	0.193
22029	2050474.	515431.	714.	-39.8	-62.6	-62.5	0.101
22999	2092115.	548871.	745.	-38.1	-61.9	-61.7	0.185
23000	2092115.	548871.	745.	-38.1	-61.9	-61.7	0.185
23001	2067880.	492088.	684.	-38.3	-60.2	-60.1	0.041
23002	2062397.	491892.	700.	-37.7	-60.0	-60.0	0.055
23003	2064278.	489529.	681.	-39.1	-60.9	-60.9	0.035
23004	2061860.	502598.	764.	-35.7	-60.1	-59.6	0.518
23005	2062846.	505951.	774.	-35.6	-60.4	-59.8	0.550
23006	2063716.	510033.	830.	-34.7	-61.3	-60.7	0.559
23007	2060361.	512210.	752.	-38.2	-62.3	-62.2	0.034
23008	2066032.	515028.	796.	-37.1	-62.5	-62.5	0.059
23009	2066335.	518635.	859.	-35.3	-62.8	-62.5	0.320
23010	2069966.	519227.	838.	-34.1	-60.9	-60.9	0.034
23011	2068221.	524686.	915.	-32.9	-62.1	-61.5	0.622
23012	2069319.	527930.	922.	-33.1	-62.6	-62.0	0.530
23013	2071779.	530923.	860.	-34.7	-62.2	-62.2	0.025
23014	2064140.	522199.	829.	-33.9	-60.4	-60.3	0.079
23015	2061423.	519388.	815.	-35.3	-61.4	-61.1	0.324
23016	2058127.	520582.	920.	-33.5	-62.9	-61.3	1.598
23017	2058305.	517304.	842.	-36.0	-62.9	-62.8	0.080
23018	2061033.	527946.	960.	-31.2	-61.9	-60.1	1.833
23019	2055500.	528188.	822.	-36.3	-62.6	-60.4	2.145
23020	2052304.	522973.	796.	-36.6	-62.1	-61.2	0.929
23021	2050379.	520602.	831.	-36.0	-62.5	-61.5	0.991
23022	2043596.	520189.	705.	-39.6	-62.1	-58.9	3.242
23023	2041154.	521169.	693.	-39.8	-62.0	-58.1	3.850
23999	2092115.	548871.	745.	-38.1	-61.9	-61.7	0.185
24000	2092115.	548871.	745.	-38.1	-61.9	-61.7	0.185
24001	2107660.	533159.	663.	-37.8	-59.0	-58.9	0.083
24002	2110756.	532189.	581.	-40.7	-59.3	-58.7	0.594
24003	2106667.	540185.	605.	-40.4	-59.8	-58.8	0.910
24004	2109589.	539978.	583.	-40.9	-59.5	-58.7	0.772
24005	2115631.	539677.	556.	-41.6	-59.4	-59.0	0.450
24006	2118299.	533133.	623.	-39.8	-59.8	-59.7	0.052
24007	2115724.	544303.	619.	-39.0	-58.8	-58.7	0.026
24008	2113141.	544984.	659.	-37.4	-58.5	-58.4	0.065
24009	2107304.	543903.	670.	-37.8	-59.2	-59.2	0.038
24010	2107179.	546670.	687.	-37.5	-59.5	-59.5	0.017

STA	XPLOT	YPLOT	ELEV	FA	SBG	CBG	TC
24011	2108577.	551411.	580.	-40.8	-59.4	-58.1	1.306
24012	2113430.	550230.	560.	-40.6	-58.5	-57.6	0.917
24013	2120088.	551024.	525.	-42.4	-59.2	-58.6	0.512
24014	2124912.	550064.	583.	-39.9	-58.5	-58.4	0.125
24015	2120147.	556670.	518.	-42.0	-58.5	-57.8	0.689
24016	2118913.	560016.	561.	-40.9	-58.9	-58.6	0.282
24017	2117759.	564563.	520.	-42.1	-58.8	-57.5	1.324
24018	2115107.	562002.	640.	-38.6	-59.1	-59.1	0.016
24019	2114201.	555296.	585.	-40.3	-59.0	-58.9	0.131
24020	2113870.	553182.	571.	-40.4	-58.6	-57.8	0.770
24021	2110813.	558741.	668.	-37.7	-59.0	-59.0	0.010
24022	2106889.	562003.	665.	-38.3	-59.5	-59.5	0.075
24023	2108239.	564376.	630.	-38.7	-58.8	-58.7	0.095
24024	2109305.	567076.	591.	-40.1	-59.0	-58.4	0.642
24025	2106664.	568376.	662.	-37.6	-58.8	-58.7	0.084
24026	2108498.	570241.	647.	-38.1	-58.8	-58.7	0.099
24027	2114538.	568883.	623.	-38.3	-58.3	-58.0	0.212
24028	2119470.	568468.	548.	-41.1	-58.7	-58.6	0.076
24029	2121839.	570738.	531.	-42.1	-59.0	-58.5	0.530
24030	2110839.	572655.	606.	-38.7	-58.1	-57.9	0.187
24031	2111369.	574697.	618.	-38.7	-58.5	-58.4	0.068
24999	2092115.	548871.	745.	-38.1	-61.9	-61.7	0.185
25000	2092115.	548871.	745.	-38.1	-61.9	-61.7	0.185
25001	2114435.	579336.	624.	-38.9	-58.9	-58.9	0.020
25002	2119588.	579578.	616.	-37.9	-57.6	-57.5	0.052
25003	2122652.	578463.	591.	-40.0	-58.9	-58.9	0.014
25004	2125376.	577384.	601.	-39.7	-58.9	-58.8	0.027
25005	2124965.	574431.	589.	-39.9	-58.7	-58.7	0.073
25006	2127309.	575972.	561.	-40.6	-58.5	-58.5	0.066
25007	2130490.	574203.	500.	-42.9	-58.9	-58.8	0.083
25008	2137177.	584509.	531.	-41.7	-58.7	-58.7	0.009
25009	2126255.	582961.	584.	-39.9	-58.6	-58.6	0.023
25999	2092115.	548871.	745.	-38.1	-61.9	-61.7	0.185
26000	2092115.	548871.	745.	-38.1	-61.9	-61.7	0.185
26001	2108999.	579277.	698.	-37.5	-59.9	-59.8	0.024
26002	2111272.	584094.	683.	-37.9	-59.7	-59.7	0.070
26003	2106965.	584914.	671.	-42.1	-63.5	-62.8	0.762
26004	2116031.	583605.	622.	-39.8	-59.7	-59.7	0.041
26005	2117254.	588491.	626.	-39.8	-59.8	-59.8	0.017
26006	2121245.	588692.	598.	-39.5	-58.6	-58.6	0.034
26007	2120362.	583807.	635.	-38.8	-59.1	-59.1	0.027
26008	2118847.	593015.	638.	-39.0	-59.4	-59.4	0.011
26009	2113983.	592192.	658.	-38.2	-59.3	-59.1	0.172
26010	2113201.	596159.	681.	-38.0	-59.8	-59.6	0.152
26011	2109829.	590462.	756.	-36.0	-60.1	-60.1	0.022

STA	XPLOT	YPLOT	ELEV	FA	SBG	CBG	TC
26012	2108763.	594865.	742.	-35.4	-59.1	-58.7	0.385
26013	2110838.	599427.	700.	-36.5	-58.9	-58.4	0.404
26014	2106437.	603233.	843.	-31.3	-58.3	-58.0	0.242
26015	2104295.	601112.	830.	-32.7	-59.2	-59.2	0.041
26016	2101681.	596694.	858.	-32.3	-59.7	-59.6	0.111
26017	2099322.	591877.	864.	-32.2	-59.8	-59.7	0.100
26018	2096429.	593505.	739.	-37.0	-60.6	-60.2	0.436
26019	2094550.	596449.	728.	-37.5	-60.8	-60.5	0.347
26020	2099115.	601492.	875.	-32.9	-60.9	-60.0	0.973
26021	2102304.	603763.	770.	-34.4	-59.0	-58.8	0.183
26022	2090919.	599022.	843.	-33.6	-60.6	-60.5	0.067
26023	2093821.	602274.	657.	-40.5	-61.5	-60.9	0.640
26024	2093951.	605589.	618.	-42.1	-61.9	-59.3	2.533
26025	2093344.	609084.	635.	-41.5	-61.8	-60.9	0.903
26026	2096422.	610516.	752.	-37.1	-61.2	-60.3	0.879
26027	2091182.	612682.	624.	-42.6	-62.5	-61.9	0.610
26028	2088157.	612417.	551.	-44.1	-61.7	-61.4	0.322
26029	2089299.	617484.	575.	-44.0	-62.4	-62.3	0.126
26030	2082746.	615022.	682.	-40.5	-62.3	-61.5	0.778
26031	2081648.	613452.	784.	-36.8	-61.8	-61.3	0.550
26032	2081347.	619279.	882.	-33.0	-61.2	-60.9	0.375
26033	2082755.	621287.	875.	-33.9	-61.9	-61.6	0.281
26999	2092115.	548871.	745.	-38.1	-61.9	-61.7	0.185
29000	2092115.	548871.	745.	-38.1	-61.9	-61.7	0.185
29001	2094241.	580275.	888.	-32.3	-60.7	-60.5	0.154
29002	2093258.	578050.	958.	-31.0	-61.6	-60.8	0.778
29003	2098947.	578836.	766.	-36.4	-60.9	-60.7	0.269
29004	2103538.	578089.	713.	-38.2	-61.0	-61.0	0.089
29005	2103670.	580348.	742.	-36.6	-60.4	-60.3	0.027
29006	2104839.	585415.	786.	-35.8	-60.9	-60.8	0.075
29007	2103151.	589998.	811.	-34.2	-60.1	-60.0	0.048
29008	2095366.	590150.	764.	-37.6	-62.0	-61.8	0.230
29009	2095580.	585817.	880.	-33.2	-61.3	-61.1	0.157
29010	2091227.	583688.	869.	-33.8	-61.6	-61.5	0.135
29011	2089489.	586815.	842.	-34.4	-61.3	-61.2	0.150
29012	2088031.	582585.	780.	-36.4	-61.4	-61.0	0.373
29013	2086570.	579265.	820.	-35.2	-61.5	-61.2	0.276
29014	2080486.	577789.	777.	-36.8	-61.6	-60.9	0.685
29015	2081194.	586715.	923.	-30.8	-60.3	-60.1	0.242
29016	2081695.	589557.	930.	-32.0	-61.8	-59.6	2.113
29017	2083293.	594370.	835.	-34.5	-61.2	-61.0	0.198
29018	2086014.	593287.	704.	-38.8	-61.3	-60.8	0.536
29019	2085372.	599258.	880.	-33.1	-61.2	-59.9	1.387
29020	2083715.	604097.	671.	-40.2	-61.7	-61.3	0.342
29021	2082249.	602417.	557.	-44.8	-62.6	-62.2	0.421

STA	XPLOT	YPLOT	ELEV	FA	SBG	CBG	TC
29022	2078456.	602915.	660.	-40.7	-61.8	-61.7	0.150
29023	2076185.	605604.	826.	-35.6	-62.0	-61.6	0.340
29024	2078013.	609106.	597.	-43.1	-62.2	-57.9	4.331
29025	2075446.	597078.	667.	-41.3	-62.6	-62.4	0.160
29026	2076478.	592383.	583.	-43.3	-61.9	-61.7	0.276
29027	2075211.	590303.	595.	-43.5	-62.5	-62.1	0.389
29028	2073182.	586946.	635.	-41.8	-62.1	-61.7	0.463
29999	2092115.	548871.	745.	-38.1	-61.9	-61.7	0.185
30000	2092115.	548871.	745.	-38.1	-61.9	-61.7	0.185
30001	2084290.	583847.	761.	-36.9	-61.2	-60.9	0.249
30002	2083322.	585265.	774.	-36.8	-61.5	-61.1	0.370
30003	2073078.	583558.	630.	-42.0	-62.1	-61.6	0.552
30004	2066488.	580845.	746.	-38.3	-62.1	-61.6	0.554
30005	2068538.	587297.	635.	-41.9	-62.2	-60.5	1.714
30006	2069493.	590287.	611.	-43.2	-62.8	-61.6	1.168
30007	2069785.	597172.	611.	-43.8	-63.4	-62.1	1.251
30008	2072206.	601950.	904.	-33.2	-62.1	-59.9	2.182
30009	2072530.	607451.	777.	-37.2	-62.0	-61.8	0.227
30010	2076505.	612016.	656.	-42.4	-63.4	-62.7	0.728
30011	2070897.	615059.	817.	-35.7	-61.8	-61.5	0.240
30012	2068702.	610974.	739.	-38.6	-62.2	-59.9	2.313
30013	2068597.	607841.	831.	-35.0	-61.5	-61.5	0.057
30014	2067589.	603868.	947.	-31.4	-61.6	-57.8	3.811
30015	2069538.	615638.	877.	-34.4	-62.5	-61.1	1.434
30016	2063476.	619994.	779.	-37.5	-62.4	-60.9	1.535
30017	2060740.	617146.	913.	-32.2	-61.4	-60.9	0.529
30018	2060330.	610917.	937.	-31.0	-61.0	-60.0	0.971
30019	2060650.	607202.	733.	-38.5	-61.9	-60.7	1.263
30020	2058454.	602280.	971.	-31.3	-62.3	-59.8	2.589
30021	2054603.	603801.	945.	-31.1	-61.3	-61.1	0.248
30022	2048883.	606485.	1006.	-28.5	-60.7	-60.6	0.092
30023	2044786.	603637.	965.	-29.1	-60.0	-59.7	0.244
30024	2043435.	599336.	1038.	-26.9	-60.1	-59.7	0.363
30025	2042450.	596421.	964.	-30.1	-60.9	-60.7	0.174
30026	2043956.	592744.	1018.	-28.7	-61.2	-60.4	0.798
30027	2051142.	594251.	995.	-30.0	-61.9	-61.4	0.478
30028	2056437.	593096.	750.	-39.9	-63.9	-63.5	0.327
30029	2062205.	595550.	669.	-41.9	-63.3	-62.9	0.403
30030	2064025.	592094.	740.	-39.1	-62.8	-62.0	0.855
30999	2092115.	548871.	745.	-38.1	-61.9	-61.7	0.185
31000	2092115.	548871.	745.	-38.1	-61.9	-61.7	0.185
31002	2058267.	584759.	724.	-40.7	-63.9	-62.8	1.104
31003	2060018.	586912.	671.	-42.3	-63.8	-62.7	1.060
31004	2055291.	586173.	661.	-44.0	-65.1	-64.7	0.407
31005	2048831.	589220.	1034.	-28.7	-61.7	-61.5	0.286

STA	XPLOT	YPLOT	ELEV	FA	SBG	CBG	TC
31006	2048307.	581461.	703.	-42.1	-64.6	-63.9	0.697
31007	2045054.	579706.	740.	-40.8	-64.4	-63.0	1.455
31008	2042106.	581595.	969.	-30.3	-61.3	-60.7	0.569
31009	2039402.	590479.	1162.	-23.5	-60.6	-58.9	1.727
31010	2036771.	589710.	972.	-29.1	-60.2	-59.7	0.542
31011	2039075.	601369.	1253.	-19.0	-59.0	-58.8	0.259
31012	2044041.	609463.	1243.	-20.8	-60.5	-60.2	0.296
31013	2039336.	615684.	1153.	-23.3	-60.2	-59.6	0.545
31014	2047111.	616535.	1313.	-17.7	-59.7	-59.0	0.712
31015	2049561.	621821.	1290.	-17.8	-59.1	-58.7	0.384
31016	2048729.	613260.	1037.	-26.7	-59.9	-59.7	0.167
31017	2054619.	609556.	831.	-34.9	-61.5	-60.8	0.634
31018	2055790.	617427.	1074.	-26.0	-60.3	-59.6	0.734
31019	2057620.	621328.	1116.	-24.6	-60.3	-60.0	0.254
31020	2057870.	623077.	1092.	-24.9	-59.8	-59.7	0.145
31021	2069451.	627149.	835.	-34.9	-61.6	-61.2	0.365
31022	2072206.	632584.	932.	-31.7	-61.5	-61.1	0.398
31023	2072732.	626393.	1208.	-22.1	-60.8	-59.6	1.150
31999	2092115.	548871.	745.	-38.1	-61.9	-61.7	0.185
32000	2092115.	548871.	745.	-38.1	-61.9	-61.7	0.185
32001	2056791.	625187.	1114.	-24.2	-59.8	-59.6	0.163
32002	2063002.	628699.	1124.	-24.6	-60.5	-60.0	0.545
32003	2067536.	635267.	1074.	-26.9	-61.3	-61.0	0.223
32004	2069773.	633305.	1166.	-23.1	-60.4	-58.9	1.530
32005	2065058.	631545.	1124.	-25.2	-61.2	-60.1	1.068
32006	2056613.	629339.	1077.	-25.2	-59.6	-59.4	0.231
32007	2061517.	635033.	1006.	-28.6	-60.8	-60.6	0.158
32008	2053726.	631082.	1213.	-20.7	-59.5	-59.4	0.143
32009	2056343.	636296.	1191.	-21.5	-59.6	-59.0	0.562
32010	2057836.	638558.	1146.	-22.5	-59.2	-59.0	0.211
32011	2059467.	641986.	1130.	-24.6	-60.7	-60.3	0.425
32012	2043090.	653974.	2313.	13.6	-60.3	-58.1	2.234
32013	2054317.	646127.	900.	-32.5	-61.3	-60.9	0.392
32014	2053672.	643466.	858.	-34.2	-61.6	-60.8	0.797
32015	2052437.	639931.	914.	-32.2	-61.4	-60.7	0.638
32016	2051118.	635047.	900.	-32.2	-61.0	-60.0	1.042
32017	2049795.	632713.	917.	-29.9	-59.2	-58.3	0.940
32018	2046357.	627170.	958.	-29.7	-60.3	-59.8	0.556
32019	2050941.	624665.	1250.	-19.2	-59.2	-58.9	0.260
32020	2030544.	589119.	1126.	-23.0	-59.0	-58.6	0.397
32021	2033623.	594259.	1283.	-17.8	-58.8	-58.0	0.828
32022	2023616.	580662.	1263.	-17.4	-57.8	-56.2	1.588
32023	2030409.	583400.	1005.	-27.2	-59.4	-58.3	1.094
32024	2034573.	582204.	1171.	-22.2	-59.7	-58.9	0.762
32999	2092115.	548871.	745.	-38.1	-61.9	-61.7	0.185

STA	XPLOT	YPLOT	ELEV	FA	SBG	CBG	TC
33000	2092115.	548871.	745.	-38.1	-61.9	-61.7	0.185
33001	2007103.	493494.	941.	-31.4	-61.5	-58.4	3.051
33002	2010112.	499395.	1144.	-23.7	-60.3	-59.9	0.391
33006	2012832.	514365.	964.	-31.7	-62.5	-56.6	5.954
33007	2013855.	511670.	975.	-30.2	-61.4	-58.3	3.154
33008	2022803.	506978.	1026.	-28.3	-61.1	-60.8	0.303
33009	2020979.	515463.	800.	-35.6	-61.2	-59.9	1.351
33010	2022996.	513534.	823.	-35.5	-61.8	-61.5	0.348
33011	2018451.	517646.	835.	-35.3	-62.0	-59.7	2.250
33015	2005533.	530169.	1550.	-11.1	-60.7	-59.7	1.051
33016	2000596.	518623.	1896.	1.5	-59.1	-56.5	2.646
33017	1997275.	516657.	2136.	8.0	-60.3	-52.7	7.648
33018	2020266.	518922.	887.	-32.6	-61.0	-59.7	1.266
33019	2023074.	521074.	917.	-31.9	-61.2	-60.8	0.440
33020	2026106.	526795.	855.	-34.1	-61.4	-60.6	0.769
33021	2023890.	528978.	948.	-31.4	-61.7	-59.0	2.748
33022	2029630.	521918.	734.	-38.6	-62.1	-61.0	1.065
33023	2029367.	528146.	836.	-34.7	-61.4	-60.9	0.517
33024	2029554.	538308.	1088.	-27.0	-61.8	-58.5	3.341
33025	2033291.	543739.	1098.	-27.0	-62.1	-57.9	4.232
33027	2031599.	535906.	1064.	-27.6	-61.6	-60.9	0.742
33028	2034009.	537330.	925.	-31.2	-60.8	-59.8	1.004
33999	2092115.	548871.	745.	-38.1	-61.9	-61.7	0.185
36000	2092115.	548871.	745.	-38.1	-61.9	-61.7	0.185
36001	2053222.	532008.	784.	-36.4	-61.5	-60.4	1.110
36002	2056799.	531178.	852.	-35.4	-62.7	-60.6	2.039
36003	2061358.	534575.	858.	-34.0	-61.5	-61.4	0.068
36004	2063566.	536802.	871.	-33.8	-61.7	-61.5	0.138
36005	2067728.	539727.	895.	-33.1	-61.7	-61.6	0.040
36006	2063919.	542959.	996.	-31.5	-63.4	-63.2	0.105
36007	2070436.	544906.	876.	-34.2	-62.2	-61.9	0.228
36008	2066747.	545952.	940.	-32.5	-62.6	-59.8	2.814
36009	2070108.	551060.	953.	-31.7	-62.2	-60.2	2.046
36010	2070089.	557944.	809.	-36.3	-62.2	-60.9	1.334
36011	2064706.	557093.	947.	-30.0	-60.3	-60.2	0.094
36012	2062481.	551332.	1084.	-26.0	-60.7	-60.4	0.348
36013	2065763.	553781.	900.	-31.8	-60.6	-59.0	1.582
36014	2060333.	548705.	1104.	-25.0	-60.3	-59.8	0.543
36015	2060962.	546448.	1018.	-28.7	-61.2	-60.8	0.407
36016	2056358.	551391.	1053.	-26.7	-60.4	-60.2	0.169
36017	2057649.	544255.	1088.	-25.6	-60.4	-59.6	0.817
36018	2053605.	539002.	997.	-28.8	-60.7	-60.4	0.358
36019	2052430.	545118.	1028.	-27.3	-60.2	-59.7	0.449
36020	2048656.	546495.	984.	-29.6	-61.0	-61.0	0.080
36021	2047164.	540701.	1126.	-24.0	-60.0	-59.1	0.944

STA	XPLOT	YPLOT	ELEV	FA	SBG	CBG	TC
36022	2043655.	535669.	1112.	-24.8	-60.3	-55.3	5.027
36023	2036481.	534347.	967.	-22.8	-53.7	-53.4	0.306
36024	2034043.	532449.	957.	-29.3	-59.9	-59.1	0.827
36999	2092115.	548871.	745.	-38.1	-61.9	-61.7	0.185
37000	2092115.	548871.	745.	-38.1	-61.9	-61.7	0.185
37001	2069304.	565518.	909.	-31.2	-60.3	-59.7	0.505
37002	2065341.	564124.	713.	-38.6	-61.4	-59.2	2.190
37003	2057014.	575104.	887.	-33.4	-61.7	-58.9	2.813
37004	2061040.	573401.	764.	-37.8	-62.2	-61.9	0.246
37005	2066590.	574180.	652.	-41.4	-62.2	-61.6	0.614
37006	2062706.	575846.	762.	-37.2	-61.6	-61.3	0.259
37007	2058444.	569207.	763.	-36.9	-61.3	-60.3	1.044
37008	2056288.	570695.	810.	-36.1	-62.0	-59.3	2.621
37009	2053123.	566500.	944.	-31.4	-61.6	-60.4	1.164
37010	2051834.	559541.	803.	-35.8	-61.5	-59.2	2.222
37011	2048769.	561829.	973.	-31.5	-62.7	-58.3	4.343
37012	2045622.	562588.	1492.	-14.8	-62.6	-57.2	5.379
37013	2038149.	556967.	2308.	12.4	-61.4	-57.4	3.948
37014	2040157.	560103.	2225.	8.3	-62.8	-58.5	4.256
37015	2045353.	554575.	1027.	-28.4	-61.2	-60.1	1.161
37016	2042914.	555299.	1183.	-24.0	-61.8	-58.4	3.375
37017	2048217.	553888.	831.	-34.3	-60.8	-58.9	1.985
37018	2045247.	550131.	908.	-31.7	-60.8	-58.8	1.929
37019	2041880.	545864.	944.	-30.9	-61.1	-60.0	1.118
37020	2043330.	543353.	984.	-29.1	-60.5	-60.2	0.360
37021	2039900.	542947.	944.	-31.0	-61.2	-60.2	0.986
37022	2036049.	539008.	920.	-32.0	-61.4	-60.5	0.912
37023	2056956.	562793.	752.	-37.7	-61.8	-61.3	0.428
37024	2060326.	563675.	700.	-39.2	-61.5	-60.9	0.660
37025	2063153.	566413.	684.	-40.1	-62.0	-61.7	0.268
37999	2092115.	548871.	745.	-38.1	-61.9	-61.7	0.185
38000	2092115.	548871.	745.	-38.1	-61.9	-61.7	0.185
38001	2032006.	574515.	1171.	-22.5	-59.9	-59.5	0.445
38002	2026628.	570684.	1318.	-17.0	-59.2	-58.6	0.524
38003	2026115.	574326.	1412.	-13.5	-58.6	-56.1	2.500
38004	2022951.	564708.	1364.	-15.1	-58.8	-58.6	0.192
38005	2017600.	558001.	1395.	-14.3	-59.0	-58.5	0.451
38006	2018625.	552175.	1178.	-22.1	-59.8	-58.3	1.484
38007	2023496.	556658.	1128.	-23.9	-60.0	-57.2	2.746
38008	2025931.	559793.	1037.	-27.8	-60.9	-57.1	3.824
38009	2023011.	560883.	1202.	-20.6	-59.1	-58.8	0.250
38010	2031423.	564826.	896.	-33.1	-61.7	-58.3	3.465
38011	2032105.	562860.	974.	-31.4	-62.5	-59.9	2.634
38012	2037625.	566546.	1167.	-23.1	-60.4	-59.7	0.770
38013	2037900.	572374.	789.	-37.1	-62.3	-60.1	2.177

STA	XPLOT	YPLOT	ELEV	FA	SBG	CBG	TC
38999	2092115.	548871.	745.	-38.1	-61.9	-61.7	0.185

The vita has been removed from
the scanned document